Fermilab Proposal No. 636

Scientific Spokesman: Irwin A. Pless
Massachusetts Institute of Technology
Telephone: (617) 253-6081
25 April 1980

NEUTRINO INTERACTION STUDIES AT TEVATRON ENERGIES USING A BEAM DUMP TECHNIQUE TO PRODUCE THE NEUTRINO BEAM

E. S. Hafen, P. Haridas, R. I. Hulsizer, V. Kistiakowsky,
I. A. Pless, R. K. Yamamoto
Massachusetts Institute of Technology, Cambridge, Massachusetts 02139

D. Brick, H. Rudnicka, A. Shapiro, M. Widgoff
Brown University, Providence, Rhode Island, 02912

T. Murphy
Fermilab, Batavia, Illinois 06510

E. D. Alyea, Jr.
Indiana University, Bloomington, Indiana 47401

G. Fujioka and others
Kobe University, Kobe, Japan

H. O. Cohn
Oak Ridge National Laboratory, Oak Ridge, Tennessee 37830

O. Kusumoto, T. Teranaka, and others
Osaka City University, Osaka, Japan

R. L. DiMarco, P. Jacques, M. Kalelkar, P. A. Miller, R. J. Plano
Rutgers University, New Brunswick, New Jersey 08903

W. M. Bugg, G. T. Condo, T. Handler, E. L. Hart
University of Tennessee, Knoxville, Tennessee 37916

T. Kitagaki, S. Tanaka, H. Yuta, K. Abe, K. Hasegawa,
A. Yamaguchi, K. Tamai, Y. Hayashino
Tohoku University, Sendai, Japan

H. D. Taft
Yale University, New Haven, Connecticut 06520

Table of Contents

		Page No.
I.	Introduction	1
II.	Physics	2
III.	Beam Dump	6
IV.	Apparatus	10
V.	Event Rates	14
VI.	Analysis	16
VII.	Cost Estimates	20
VIII.	Summary	21
	Appendix I, Active Shield	22
	Appendix II, Experimental Equipment	35
	Appendix III, Event Rates	40
	Appendix IV, Technique	46

Neutrino Interaction Studies at Tevatron Energies

using a Beam Dump Technique to Produce the Neutrino Beam

We propose to search for τ mesons produced by neutrino interactions with matter. Besides finding such a reaction, we expect to be able to measure the lifetime of the τ meson. We expect that 2,200 τ mesons will be produced in our apparatus for 2.5×10^{18} protons on target. The neutrinos will be produced by a beam dump technique. The neutrino beam so produced should contain equal mixtures of ν_μ, $\bar{\nu}_\mu$, ν_e, $\bar{\nu}_e$ while the ν_τ, $\bar{\nu}_\tau$ components should be $\sim$ 10% of the other components. We should therefore have a large sample of interactions induced by muon neutrinos and electron neutrinos. This sample will allow a detailed check of μ-e universality at a new energy range. We may also get a sample of charmed events and finally, if there are new particles with short half-lives and a unique decay mode, we may have a chance to see them.

Our detection apparatus consists of a visual detector and a downstream multi-particle spectrometer. The visual detector is a rapid cycling (20-40 Hertz) freon bubble chamber. Since the active liquid is nonflammable and nontoxic, this chamber can be built and operated by the experimenters and thus eliminate the need of a Fermilab crew or special safety precautions in the experimental area housing the device. We will have γ ray detection, μ e identification, and good momentum measurements on charged particles.

A short period of testing and debugging the equipment will be needed before the main run of 2.5×10^{18} protons.

Neutrino Interaction Studies at Tevatron Energies using a Beam Dump Technique to Produce the Neutrino Beam.

I. Introduction

Beam dump experiments have been performed at CERN and the results indicate that electron and muon neutrinos are produced in equal numbers. The source of these prompt neutrinos is assumed to be the production and leptonic decay of charmed particles. For the purpose of this experiment, we assume the existence of the F-meson and its decay into a τ neutrino and a τ meson followed by the decay of the τ meson into a τ neutrino. Hence, we assume a neutrino beam composed of a mixture of μ , e, and τ neutrinos which will be used to produce interactions in our detector.

In Section II, we discuss the physics of this experiment; in Section III we describe some beam dump techniques; in Section IV we give the details of our experimental apparatus; in Section V we calculate our event rates; in Section VI we present our analysis techniques and our estimated backgrounds; in Section VII we pass quickly over our cost estimates; and Section VIII is our summary.

II. Physics Objectives

One of the major thrusts of this experiment is to establish the existence of a neutrino whose interaction with matter produces a τ meson. At the same time we will have a measurement of the τ meson lifetime. We should produce 2200 τ mesons in our detector and about half of these should be useful for analysis. This is discussed in detail in section V Rates and section VI Analysis Techniques. We should be able to measure the τ lifetime to better than 30%.

Our detector consists of two parts, a high resolution visible target and a downstream spectrometer. The first component will detect the production and decay points of short lived objects, while the downstream spectrometer will analyze the decay products of the τ meson. The details of the equipment will be discussed in Section IV.

The τ meson was initially discovered by Perl et al at Spear (Perl et al, Phys. Rev. Lett, 35 (1975) 1489) and has been since confirmed by many experiments, both at Spear and Petra. To date all information on the τ meson has been obtained at e^+e^- colliding beam accelerators. The available data on τ mesons can be summarized by the following:

Mass	1800 MeV/C^2	
Life time	$< 3.5\ 10^{-12}$ sec (measurement)	(Pluto collaboration DESY Report-DESY-78/25)
	$\approx 2.5 \times 10^{-13}$ sec (theoretical)	
Spins	1/2 (DELCO Y. S. TSH1 SLAC Preprint-SLAC Pub-2105 1978)	
Mass τ Neutrino	< 250 MeV/C^2 (DELCO SLAC Preprint SLAC-Pub-2127)	

Branching Ratios for τ.

$\tau^- \rightarrow \nu_\tau + e^- + \bar{\nu}e$	18. %	(1)
$\rightarrow \nu_\tau + \mu^- + \bar{\nu}_\mu$	18. %	(2)
$\rightarrow \nu_\tau + \pi^-$	10. %	(3)
$\nu_\tau + \rho^-$	21. %	(4)
$\nu_\tau + A_1^-$	10. %	(5)
$\nu_\tau + N\pi$	23 %	(6)

All existing data on the τ is consistent with the τ being a heavy lepton with its own unique neutrino (sequential heavy lepton) or a heavy lepton with the same lepton number as the electron (e-related ortho lepton). The currently favored assumption is that the τ is a sequential heavy lepton. The reason for this prejudice is that the allowed decay for an e-related ortho lepton $\tau^- \rightarrow e^- + \gamma$ is not observed at the 3% level. Hence, either the τ is a sequential lepton or there is another mechanism which suppresses this decay mode. For the purposes of the following discussions we will assume that the τ is a sequential heavy lepton.

Beam dump experiments have been performed at CERN and the results indicate that electron and muon neutrinos are produced in equal numbers. The source of these prompt neutrinos is assumed to be the production and leptonic decay of charmed particles. In the calculations for our experiment we assume the existence of the F meson and its decay into a τ neutrino and a τ meson. The τ meson then decays into another τ neutrino. These τ neutrinos are then allowed to interact with our detector to produce τ mesons:

$$\nu_\tau + N \rightarrow \tau + \text{anything}$$

With approximately 1000 detected events we will be able to check the branching ratios of the τ meson which insures that the sample of events we

finally select are mainly τ meson decays.

This measurement will establish the existence of a neutrino interaction that produces τ mesons. As will be discussed in Section VI, these events not only establish the existence of a neutrino that can produce τ mesons but these events will be used to measure the τ meson life time.

If either the τ is an e-related ortho lepton or if the e neutrino and the τ neutrino have non-zero small masses and there is large mixing, then one might see evidence for either of these two cases in our data, or comparing our data with data taken at a different distance. However, we believe the main point to emphasize at this time is the discovery of an appropriate neutrino and then investigate its properties.

This experiment should contain up to 20,000 ν_e induced events and hence will furnish for the first time a large sample of this reaction. We will also have an equal number ν_μ induced reactions. Therefore, one will be able to study, in great detail, the similarity or differences between these two reactions. If we assume μ-e universality, then the two reactions should be identical. This has not been verified in the energy region available to this experiment, and the proposed measurement will constitute a new check of theory.

Since we have a high resolution visible target, we will be able to explore not only the production of τ mesons but also the production of the by now conventional charmed mesons. In addition, if there are other objects with lifetimes $\sim 10^{-13}$ seconds that have unique decay modes, we have an opportunity to discover them.

In the three topics discussed we should again emphasize that because of our visible target and downstream spectrometer we will be able to measure the momentum of all long lived charged particles, the energies of all gamma rays,

and identify electrons and muons with high efficiency. We will also identify K mesons and antiprotons for a subset of the produced particles. The only produced particles for which we will have little or no direct measurements will be neutrons, K_0 long, and neutrinos. This detailed information will be invaluable for identifying the decay modes of the τ meson, comparing ν_e interactions with V_μ interactions, finding charmed mesons and baryons and looking for new phenomena.

III. Beam Dump Technique

In concept, a beam of neutrinos produced by a beam dump technique is very simple. You dump $\sim 10^{13}$ 800 GeV protons on a tungsten target and follow that by 400-800 meters of iron. This ranges out all muons and you are left with a clean beam of neutrinos. The problem with this solution is two fold; first, the cost and second, the solid angle available for the detector. Hence, most beam dump designs consider active magnetic elements that sweep out the high energy muons and only limited shielding to range out the low-energy muons. We have considered a number of magnetic beam dump configurations and they are described in Appendix 1 -

. Calculating the number of muons passing through a beam dump configuration and impinging on a detector is very difficult and not very precise. We have independently written three programs and compared their predictions for identical geometries. We have also compared our results with other groups. The predictions range over three orders of magnitude. However, it seems that if one program predicts that a certain beam dump is better than another, most programs support that prediction. We have approached this problem from several points of view. The first is an attempt to design a system that is compatible with the 15' chamber. This means designing a system with both chambers on the same line. We have found this to be possible. In fact, many configurations are compatible. There always seems to be two positions in a design where the muon flux is acceptably low for both the 15' and our detector. Depending on the design, the flux of τ neutrinos in our detector can vary somewhat.

The second approach is to optimize the beam dump so as to take advantage of the properties of our high resolution detector. As described in detail in Section IV, our high resolution detector is a twenty-forty Hertz freon bubble chamber. Hence, since we can allow 50-100 noninteracting muons per expansion and since with a 10 second flat top we can take 200-400 expansions, we can stand of the order of 10,000 -40,000 muons per 10^{13} incident protons.

Appendix 1, Active Shield, describes the configurations we have studied, and all configurations would seem to be satisfactory for our chamber, given the number of muons we can tolerate per 10^{13} protons. Hence, even if all calculations are wrong by one or two orders of magnitude, the muon background from a reasonably designed beam dump should not affect our experiment if we permit rapid cycling of our detector. However, it should be noted here that rapid cycling of our detector is incompatible with the 15' chamber mode of operation.

In private discussions about the muon backgrounds for our experiment, two questions always came up. Hence, it seems reasonable to discuss them here.

The first is how many noninteracting background muons per picture could we tolerate compared to the number of background muons per picture the 15' could tolerate. The answer to that is as follows.

We will assume both the 15' and our detector use the same size film, namely, 70mm. That is, the image of each chamber on film is a circle 70mm in diameter. We also assume that the diameter of the image of a bubble on film is the same for the two chambers. We note here that since the 15' requires a greater depth of focus, the image size of a bubble for the 15' will, in fact, be larger than the image size for our detector.

The sketch below shows what you might expect to see on the 15' film compared to what you might see on our film when you have twenty muons passing through both detectors. We have assumed no magnetic field.

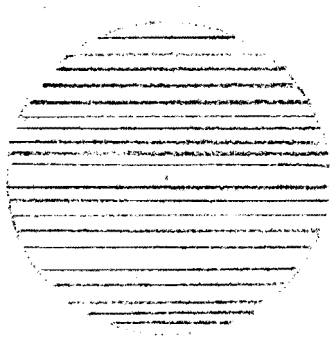

15'

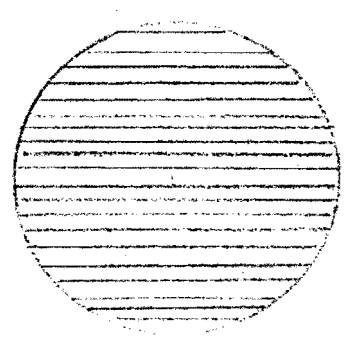

our detector

As might be suspected, the images on film (under our assumptions) are identical. I wish to emphasize (a point missed by many physicists who are not familiar with bubble chamber analysis) that all the visual information in a bubble chamber experiment is contained on the film image. Hence, given that the images of the tracks on film have the same width, the area obscured is the same for both films for the same number of tracks. Turning on the magnetic field will add curvature to the tracks. For the same muon momentum spectrum, the tracks on the 15' film will have smaller radii of curvature than on the film of our detector. Since most of the background muons will have 5 GeV/c momentum or higher, and hence tranverse essentially the whole chamber, the confusion on both films will still be the same. Note that within a region of $\sim$ 2cm from the vertex of an event (the portion of an event that is interesting for this experiment), the magnetic field has a negligible effect on the appearance of the event. This is due to the fact that the deflection of a track is proportional to L^2. Therefore, both the 15' and our detector can stand the same number of background muons per picture. However, our detector can reduce any background by taking many expansions per acceleration cycle.

The second question asked is how do we expect to be able to operate at a distance of 50 meters from the beam dump while the 15' plans to be at a greater distance. The answer is indicated in the following sketch:

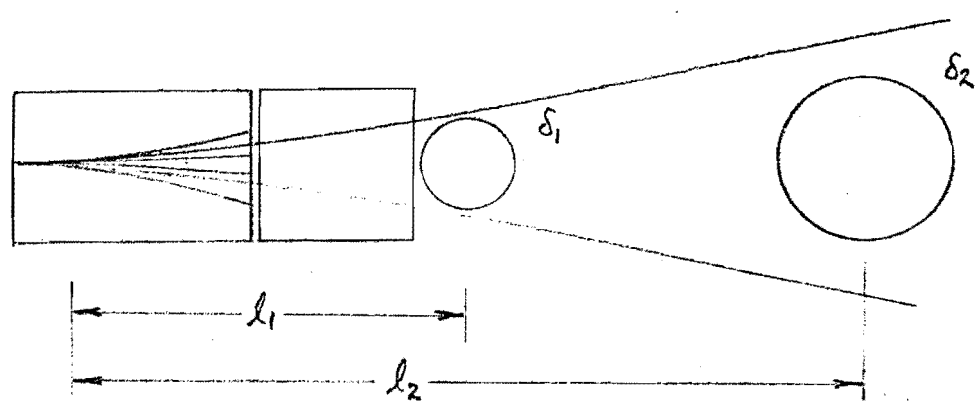

If the rays shown are the extreme muon rays (i. e. highest muon momentum at the highest $P_{\perp}$), then if $\frac{\delta_1}{\ell_1} = \frac{\delta_2}{\ell_2}$, then the probability of a muon scattering into our detector is similar to the probability that the same muon will enter the 15'. Hence, if the above criteria is satisfied, the background muon flux in our detector will be similar to the background muon flux in the 15'. The beam dump designs described in Appendix 1 - Beam Dump - satisfy the above criteria. Note the question of band pass problems must be treated separately; we discuss here only multiple scattering or deep inelastic scattering.

Finally, we have investigated the problem of fast neutrons. In all the proposed designs, the number of fast enutrons that get through the shield are completely negligible. However, thermal neutrons may be a problem and therefore we propose to surround our detector with a block house made of one meter thick concrete shielding blocks.

IV. Apparatus

Our proposed apparatus consists of two components. The first is a high resolution vertex detector and the second is a multiparticle spectrometer. The proposed high resolution vertex detector consists of a bubble chamber in the form of a cylinder 36 inches in diameter and 24 inches deep. It will be filled with a standard freon (such as F-13 B1) which operates at 80-90^0 F with a pressure of 200-300 PSI. It will be designed to operate at a cycling frequency of 20-40 cycles per second. The design will follow along the same lines as the chambers built at SLAC. It will be designed to fit into the current 30" magnet which will soon have a new superconducting coil furnishing a 33 kilogauss field.

Although a careful, complete cost analysis for this device has not been made, a ball park figure of $200,000 has been established. This estimate includes the chamber body, window, temperature control and expansion system. It does not include magnet, cameras or flash system, all of which can be taken over in great part from the current 30" chamber.

Since Freon is non-combustible and non-toxic, there are no special safety problems associated with this chamber. Hence, it is a quite appropriate device to be user owned and operated. Since the cost of this chamber is considerably less than 10^6 dollars, it is quite reasonable to consider its construction for use in a limited number of specific experiments, rather than as part of a major laboratory facility to be maintained and operated by the laboratory over a long period of time.

The second part of our detector is a downstream multiparticle detector. It will consist of proportional wire chambers, drift chambers, CRISIS, and a muon detector. Most of this would consist of the equipment that will be used

for E565 and E570. Any modifications to this equipment will be based on our experience with E565 and E570.

A schematic for the experiment is shown in Appendix II - Apparatus.

The bubble chamber will be designed using the experience and advice of SLAC. Careful attention will be paid to the optical system so as to achieve the highest possible optical resolution. Freon is a particularly suitable choice for a rapid cycling bubble chamber, as the spurious boiling is low and there is a large difference between the refractive index of the gas and liquid, and hence one can photograph small bubbles. Appendix II lists the properties of various freons.

Freon F-13 B1 is a particularly interesting liquid. The density is 1.5, the radiation length is 11cm and its interaction length is 82 centimeters. Hence, this liquid allows good optical resolution, excellent gamma ray detection, excellent electron identification and reasonable momentum resolution. These points will be discussed in Section VI - Analysis Techniques.

If the chamber has to be used in the rapid cycling mode (to decrease the number of background muons in each picture) then there will have to be an interaction trigger to control the camera flash lamps and film advance. This trigger could be very simple. The proposal is to surround the chamber with a Barrel Hodoscope of scintillation counters, which can be programmed to fire the chamber lights when charged particles leave the downstream part of the chamber and no charged particles enter the upstream part of the chamber. We expect about 80,000 neutrino induced interactions in the bubble chamber for a run of 2.5×10^{13} protons on target.

Even if the false trigger rate is twenty times the true trigger rate, this is an exposure of 1.6×10^{6} pictures. This magnitude is a practical

number to scan, and is not any different from the number of pictures taken in large bubble chamber experiments in the recent past. A test run will determine how to define the downstream and upstream part of the chamber so as not to lose any real events and still keep the false trigger rate low. Since the time resolution of our scintillators can be of the order of a few nanoseconds, and we are talking of 50-100 muons over a two millisecond spill, loss of events due to accidental coincidences is not a problem. The major source of false trigger should come from neutrino interactions in the magnet iron that enter the bubble chamber in the "downstream" part of the chamber, and hence cause a trigger. Our crude estimates indicate that such a false trigger rate should be less than five times the true trigger rate. We will have upstream and downstream PWC chambers, and, if necessary, we will use the PWC information to require that actual tracks emanate from the chamber liquid in order to activate the trigger. Such trigger logic is currently being used in the SLAC Hybrid Spectrometer facility. At SLAC, the false trigger is less than the true trigger rate. We, of course, do not expect to do that well, but the addition of the PWC information into the trigger should reduce our false trigger rate if our crude estimate is grossly wrong.

As stated before, we will use the current equipment associated with the Fermilab Hybrid Spectrometer. The one new piece of equipment will be a muon identifier. We will use the same type of design that the EMI group at M. I. T. has developed. This consists of two layers of steel and four drift chambers. From the EMI's experience, such a muon detector will have a very high efficiency for identifying muons and be relatively inexpensive. Based on previous M. I. T. experience, this system should cost about $60,000. This does not include the cost of steel or the cost of any on-line computer needed to process the data. However, it does include all the electronics for the 320 wires involved.

Appendix II - Apparatus contains our discussion of the charged particle momentum measurement, which is better than 8%, and our electron identification probability, which is greater than 95%.

This apparatus can be built and operated by the universities and present no special demands on Fermilab operation support. That is, our requirements are the same as a counter experiment. We require no special crew to operate our equipment. The equipment cost (except for the beam dump and active shield) is also commensurate with any counter experiment.

V. Event Rates

Since a beam dump experiment represents a source of limited volume (a few centimeters in diameter by 50 centimeters long) one can increase the flux of neutrinos through a fixed size detector by moving the detector closer to the beam dump. Conversely, if you have two detectors of different size, moving the smaller closer to the dump will tend to equalize the flux passing through the two detectors. The following sketch demonstrates this point.

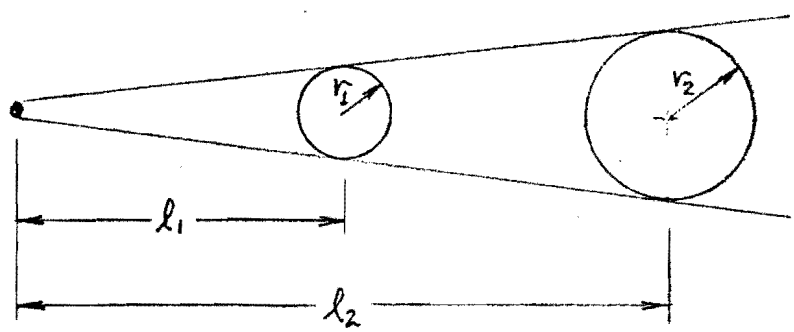

If $\frac{\ell_1}{\ell_2} = \frac{r_1}{r_2}$ (as shown in the figure, the two detectors have the same flux passing through them. In this case, if detector 1 has density ρ_1 and detector 2 has density ρ_2, then the ratio of the produced events in the detector is $\frac{r_2\ \rho_2}{r_1\ \rho_1}$ and <u>not</u> the ratio of the masses of the detector. In general the ratio of produced events in each detector will be <u>about</u> (but <u>not</u> exactly) $R = \frac{r_2{}^3\rho_2}{\ell_2{}^2}\ \frac{\ell_1{}^2}{r_1{}^3\rho_1}$.

If we take as a specific example

$r_1 = 1.5$ feet	$\rho_1 = 1.5$	$\ell_1 = 50$ meters	(our detector)
$r_2 = 6$ feet	$\rho_2 = .75$	$\ell_2 = 250$ meters	(15' bubble chamber)

$R = 1.28$

Hence, the 15' would have, under these assumptions, only 28% more events

produced in its volume as would be produced in our detector. The reason the above calculation is not precise is because the neutrino intensity is not isotropic and drops off at angles away from zero. We do the proper calculation in Appendix III - Event Rates. The correct calculation yields a ratio of 1.5.

Our basis for calculating event rates is TM-848 January 28, 1979 by S. Mori and the letter dated 3 April 1980 from J. K. Walker. As seen from the letter (enclosed as Appendix III - Event Rates) a new memo, TM-953, is being written to cover the question of neutrino flux in detail.

Our calculation is done by projecting the silhouette of our detector onto a plane at 250 meters. We can then use the S. Mori spectrum to integrate over our detector (and the 15' bubble chamber). Appendix III - Event Rates - shows the details of these calculations.

The results are that 1467 τ^- events and 733 τ^+ events will be produced in our detector for 2.5×10^{18} protons on target (with our detector at 50 meters). Hence we expect a total of 2,200 τ events to be produced in our detector. We have used a density of F13-B1 to be 1.5 gm/cubic centimeter. If we assume the 15' chamber to be a sphere 12 feet in diameter filled with a hydrogen-neon mixture with density .75 grams/cubic centimeter, then we calculate that 3,300 events will be produced in this chamber (at 250 meters).

In Section VI - Analysis Techniques we describe what fraction of these events are located in the scanning and measuring phase of this experiment.

VI. Analysis Technique

The basic analysis problem in this experiment is to locate on the film short tracks with kinks. Scanning for such tracks is very difficult and tedious. The technique proposed here is to measure the impact parameter of each track with respect to the event vertex. The following sketch shows the basic parameters:

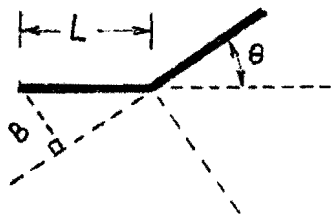

θ is the angle that the decay product of the τ makes with the τ line of flight. L is the track length of the τ and B is the impact parameter. Note that $B = L \sin\theta$. If $\frac{B}{\delta B}$ is small, then one cannot detect the τ decay. Hence, for the purpose of this analysis, we require $\frac{B}{\delta B} > 2$. If we require $\frac{B}{\delta B} > 3$, all the concepts of this analysis remain valid; it is just that the total analyzable sample is reduced in size.

The error on B is due to basically the precision of measurement. Given a bubble image on film, one can locate the center of that bubble to about 1/5 - 1/10 the bubble diameter. However, there is an intrinsic lower limit of 1-2 microns on film. This is due to the combination of measuring machine error, film grain size, and asymmetric illumination of the bubble. As is shown in the analysis appendix, we have taken the precision of measurement of two microns on film. Our analysis strategy would be to measure all tracks, as close to the vertex as possible, and then calculate B. For a neutrino experiment, the vertex should be well defined with the intrinsic error of 2 microns. For reasonable track lengths, the total error on B would be just $\sqrt{2}$ greater than this. As can be seen in the appendix, we have generated Monte-Carlo events for the production and decay of $\tau^{\pm}$ mesons using

a value of 2.8 microns for δB and plotted $B/\delta B$.

We find 43% of the events have $B/\delta B > 2$. We have also estimated how many events in the 15' would have $B/\delta B > 2$. To make this estimate we assumed the magnification for the 15' was 48 (compared to 12 for our detector) and that the precision was 3 microns (instead of the 2 microns for our detector). The reason for the larger error for the 15' is that the image of the bubble will have twice the diameter for the 15' as for our detector (note that the circle of confusion is proportional to the square root of the depth of focus which is a factor 4 larger than our detector). Hence, we assume a 50% greater error for the 15' measurements (not a factor 2). We calculate that under the 15' conditions only 4.5% of the events will have a $B/\delta B>2$. This calculation emphasizes the need for high resolution optics, high precision measurements, and the need for the demagnification from space to film to be as small as possible. For example, if our actual precision is 4 microns instead of 2 microns, the percentage of detected events drops from 43% to 8.6%, while the percentages for the 15' go from 4.5% to 0.9%. In this extreme situation, we would detect about 189 events while the 15' would detect about 29 events.

If we assume 43% of the events are detected (which we believe will be the actual case), then we should detect about 946 events. Given these events, we want to establish two points. First, the sample is indeed a sample of τ mesons, and second, to determine the τ lifetime. Since our equipment can identify π's, μ's, γ rays, and electrons, we can compare the branching ratios of our sample to the known branching ratios of the τ meson. This will establish whether or not our sample is indeed a sample of τ mesons and that we have shown that neutrinos do indeed produce τ mesons.

We have two ways to measure the lifetime of the τ meson from our data. We could select a subsample of our events in which we identify the two reactions:

$$\tau \rightarrow \pi + \nu$$

$$\tau \rightarrow \rho + \nu .$$

For these events, we can calculate the lab momentum of τ and hence calculate a proper time for each event. From the distribution of proper times, we can estimate the lifetime of the τ meson. This method has two difficulties. The first is the well known ambiguity in calculating the lab momentum of the τ and the second is the sensitivity of these calculations to measurement errors. However, it is possible to use this data to get an estimate of the lifetime. This is shown in Appendix IV.

The second technique is a statistical technique which is also described in the appendix. The basis of this technique goes as follows. If we knew the number and laboratory momentum spectrum of our τ mesons, we could calculate the laboratory length distribution, including the $B/\delta B$ cutoff as a function of the lifetime of the τ meson and fit the calculation against the measured events. If we only knew the spectrum and not the initial number, we would make a double fit on number and lifetime. This is demonstrated in the appendix. In fact, we do not know the number or spectrum, but we do know the spectrum (and number) of the muons and electrons produced by charged current interactions of ν_μ and ν_e in our chamber. If we use the S. Mori spectrums and calculate the laboratory momentum spectrum of the τ mesons, we find that the spectrums differ. However, if we match the laboratory length distribution of the τ mesons (with a cut on $B/\delta B > 2$) with that predicted from substituting the μ meson spectrum for the τ meson spectrum, we get good values for the τ lifetime. This is demonstrated in the appendix. Hence, it seems that using the measured μ meson or electron spectrum from charged current events will allow us to get a very reasonable measurement of the τ lifetime.

Another check on the existence (and number) of the τ meson in our sample is to check the ratio of μ, e charged current events to neutral current events. Any excess of neutral current events over that predicted by the number of charged current events can be attributed to the existence of τ mesons. A similar analysis might be attempted by looking at events containing leptons which have a large P_T imbalance. The

τ meson would exhibit itself as a peak at large P_T imbalance. We surely have the resolution to make the measurements; the only question would be one of signal to noise.

Since our technique requires measuring every event carefully, we will have excellent data on ν_e and $\bar{\nu}_e$ interactions.

There are two main sources of backgrounds to this analysis. They are ordinary strange particles whose decay produces a measurable impact parameter and secondary interactions which will also produce measurable impact parameters.

We expect to produce 2,200 τ mesons and we expect to produce 80,000 muons or electrons. We expect strange particle production in about 10% of our events. Hence, we will produce about 4 strange particles for each τ meson produced. Since the lifetime of these strange particles is so long, in order to decay close to the vertex, they have to be low energy and, hence, have low energy secondaries. Therefore, not very many of these strange particles will decay close to the vertex. For those that do, a cut on low energy secondary particles will eliminate most of the strange particles without affecting the τ meson sample very seriously.

The interaction length for F13 B-1 is 82cm. The average number of charged tracks should be $\sim$ 6 per event since most of the events are at 100 GeV or lower. Hence we can expect about one event in fourteen will have an interaction within one centimeter of the vertex. The events will sometimes identify themselves either by their multiplcities or the boil of protons from the nuclei in the freon. In any case, we can make an accurate correction to the data sample by measuring the interactions far from the vertex and making the usual extrapolation to the vertex and following this by the appropriate subtraction.

VII. Costs

It is not possible, at this time, to properly identify all the relevant items and their costs. However, there are some known items and some guesses on costs. They are as follows.

Experimenters Responsibility:

Bubble chamber	$ 200,000
Electronics and drift chambers for muon detector	60,000
Trigger counters and electronics	20,000
Film and development	????

Fermilab Responsibility:

Beam dump and active shield	????
Iron for muon detector	????
Laboratory building	????
30" Bubble chamber magnet and super-conducting coils (to be loaned to experimenters)	????
30" 70mm camera (to be loaned to experimenters)	????
30" Flash lamp electronics (to be loaned to experimenters)	????

This list is obviously neither complete nor exact. However, we believe all the main components are listed and hence the ball park scope of the program is indicated.

VIII. Summary

We propose a beam dump experiment to establish that τ mesons can be produced by neutrino interactions and to measure their lifetime. The technique is a rapid cycling (20-40 Hertz) freon filled bubble chamber followed by a multiparticle spectrometer. Since this type of liquid in nonflammable and nontoxic, it can be built and operated by the experimenters. We expect to produce, 2,200 τ mesons in our device and detect over 40% of them. In addition, this experiment should have 20,000 ν_e and 20,000 $\bar{\nu}_e$ induced reactions in the film. We should also detect a similar number of ν_μ and $\bar{\nu}_\mu$ induced events. These events will enable us to test e π μ universality in a new energy range with good statistics. In addition, if there is any new particle produced by neutrinos with a short half life and a unique decay mode, we may be able to detect it. Finally, we should have a sample of regular charmed particles in our data. All our estimates are based on 2.5×10^{18} protons on target.

Appendix 1: Active Shield

The design of an active shield for the beam dump experiment usually requires a suitable configuration of large iron (or superconducting) magnets along with some iron blocks of sufficient size to absorb low momentum muons that are swept in by inverse bending in return yokes. Four such configurations were examined using three different computer programs which calculate the number of muons that will enter the detector. These programs include the effects of deep-inelastic scattering of the muons in the material of the active shield.

Design-I

The first such design (labeled I) is shown in fig. I. It consists of a 22 K Gauss magnet, 30 meters long and 4.8 meters high, followed by an iron block 45 meters long. The detector (in this case the 15' bubble chamber) is at a distance of 250 meters from the dump. An iron shield 15 meters long and 3.6 meters high is placed in front of the chamber to act as absorber for those low energy muons escaping the first two components of the active shield.

Table (1) gives the results of the calculation. The values obtained from the three programs agree with each other and help determine the relative factors involved in the different normalizations used in the three programs. This also helps us compare our results with calculations of other proposals using the 15' chamber as detector.

Design II

Design II is essentially the same as design I with one major difference. The 45 meter iron absorber is now replaced by a 35 meter absorber, as shown in Fig. II. The 36" chamber is placed immediately after this iron shield, which serves to absorb the low energy muons that would have otherwise entered the chamber. Following the 36" chamber is another iron-absorber 10 meters long. The 15' chamber is at the same position as in design I.

The muon background for this configuration is also given in Table (1), both at the 36" chamber and the 15' detector. The background at the 15' is lower than that of design I and at the 36", it is about .5 muons per 10^{13} protons.

Design III

Fig. III shows the active shield in this design. It consists of four different magnets with field strengths as shown. A cross sectional view (facing beam) of these magnets is given in the same figure. The space in the center of the iron is filled with concrete to act as an absorber.

Calculations of the muon background are given in Table (I) for the 15' chamber as well as the 36".

Design IV

This design, shown in Fig. IV, has a superconducting first magnet with field strength equal to 40K Gauss. This very strong field gives the beam an initial large bending and serves to remove the high momentum muons away from the beam axis. Design IV is very similar to III; however, the size of the magnets has been made much larger.

The values for the muon background for these designs are also given in Table I.

Table II gives the weight of iron used in the various designs and Fig. V gives the typical energy distribution of muons entering each bubble chamber.

A note on the computer programs

The basic technique used in all three computer algorithms for calculating the number of background muons entering the detector is the following.

A first pass is made to determine the undeflected trajectory of a muon of known momentum through the entire active shield down to the plane containing the

center of the detector. It is now assumed that a deep inelastic scattering can occur at any point along this original trajectory. The scattered muon will have an energy E' & angle θ within the allowed kinematical limits of deep inelastic scattering. This E'-θ space is now scanned - i. e. muons with different E' and θ values are swum down to see if they hit the detector. If a hit is obtained then the probability of producing a muon with its value of E' & θ is obtained by using a suitable formula [Brasse et al. (1) or Gordon et al(2)]. Any number of such deep inelastic scattering contributions can be computed along the trajectory and an average determined. This "hit-probability" is now multiplied by the probability of producing a muon of the original trajectory using the formula of Stefansky & White (3) and the resulting quantity is integrated over the entire production spectrum of the muons.

Algorithm I considers only one deep inelastic scattering per trajectory. The angle θ giving a hit for a chosen value of E' is now determined and an integration is performed using three different values of E'.

Algorithm II spans the entire E'-θ space using a small step size for both variables and sums up the probability from all the hits. The range for E' is $0 < E' < E$ where E is the energy of the incoming muon and the range of θ is taken to be 20^0. Deep inelastic scattering is computed at many points along the trajectory.

Algorithm III first determines a reasonable smaller range for E' by determining an E'_{min} which is the energy required for the scattered muon to emerge out of the active shield. Knowing E'_{min} and E'_{max} ($E'_{max} = E$) a range for θ is computed. This θ -range is now spanned and trajectories are swum for energy E'_{min} and E'_{max} from which the correct E' value for obtaining a hit can be computed. This method requires much less computer time than Algorithm II and is equally accurate. Here also the scattering is computed at many points along the trajectory.

The Superconducting Magnet

Fig. VI shows a preliminary design of the superconducting magnet used in some of the active shield designs discussed earlier. The figure shows one-quarter of the magnet facing the beam (z-direction), with x and y being the vertical and horizontal directions respectively.

A standard program called TRIM was used to calculate the field strengths and the forces on the coils. The results of this calculation are shown in Table (3). In order to achieve a field strength of 40 KGauss in the center (near the origin of the axes), it is required to operate the magnet at 0.4×10^6 Amp-turns. The field strengths at other locations in the magnet are given in Fig. VI. For such a magnet the force on the coil is about 6.2×10^5 N/m and is roughly the same as that in the 30" magnet. The amount of superconductor required is also the same as the 30".

Being very similar to the 30" magnet we would expect the magnet coil to cost about $350,000, this being the cost for the 36" coil. This design is stable against radiation quenching.

Conclusion

In this appendix we have shown that an active shield can be constructed to remove practically all the muons emerging from the beam dump. In particular, designs II and IV can be used to do two experiments (one with the 30" and the other with the 15' chambers) simultaneously since both these designs give very little background muons in either chamber. We have also shown how the superconducting magnet used in design IV can be constructed. Finally, it is worth pointing out that design IV requires only half as much iron as that of designs I and II.

References:

(1) F. W. Brasse et al., Nucl. Phys. B39, 421 (1972).

(2) B. A. Gordon et al., Phys. Rev. D20, 2645 (1979)

(3) Stefansky & White, FN-292, 1976.

Fig-I

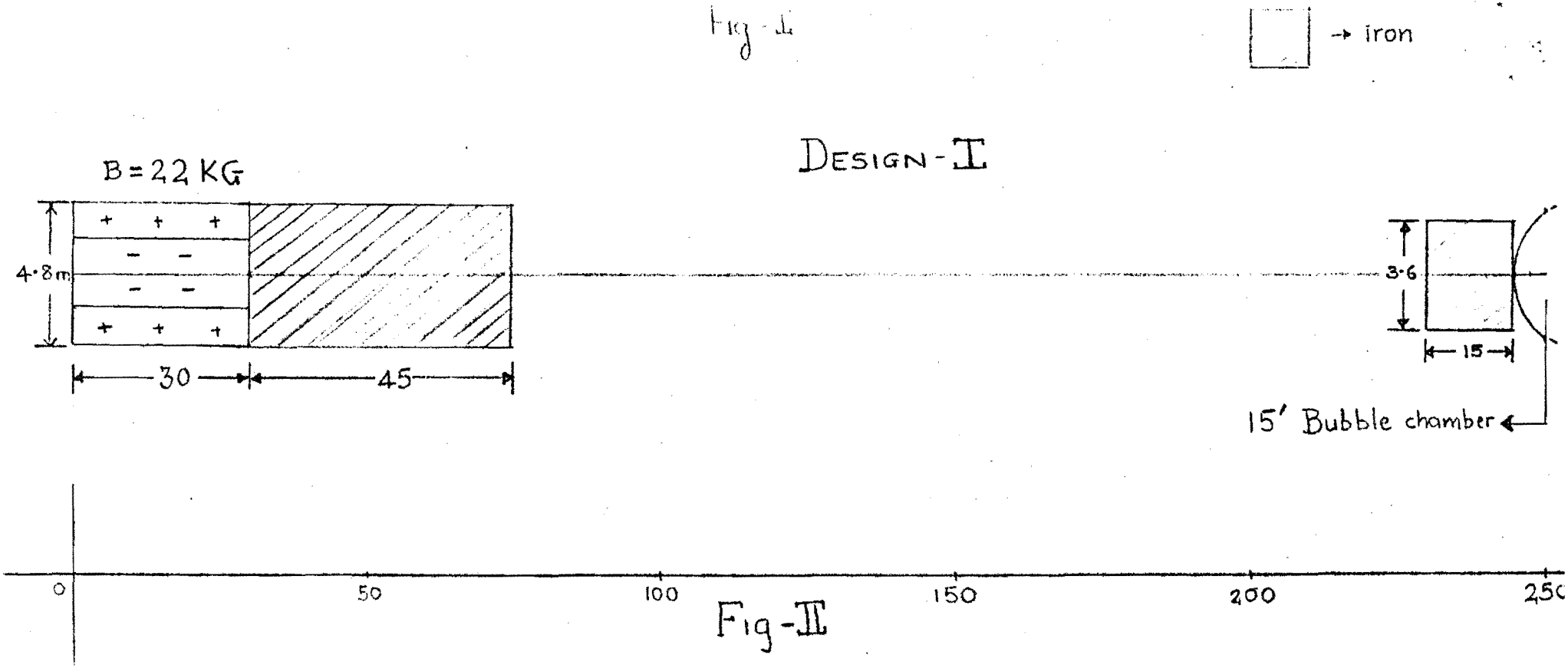
→ iron
DESIGN-I
B=22 KG
4·8m
30
45
3·6
15
15′ Bubble chamber
0
50
100
150
200
250

Fig-II

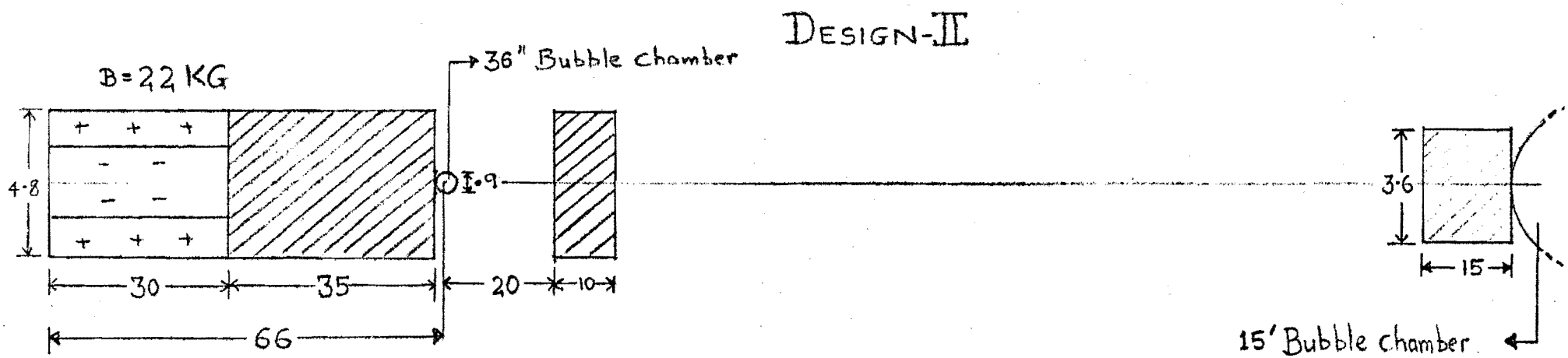
DESIGN-II
B=22 KG
→36" Bubble chamber
4·8
1·9
30
35
20
10
66
3·6
15
15′ Bubble chamber

Fig III Design - III

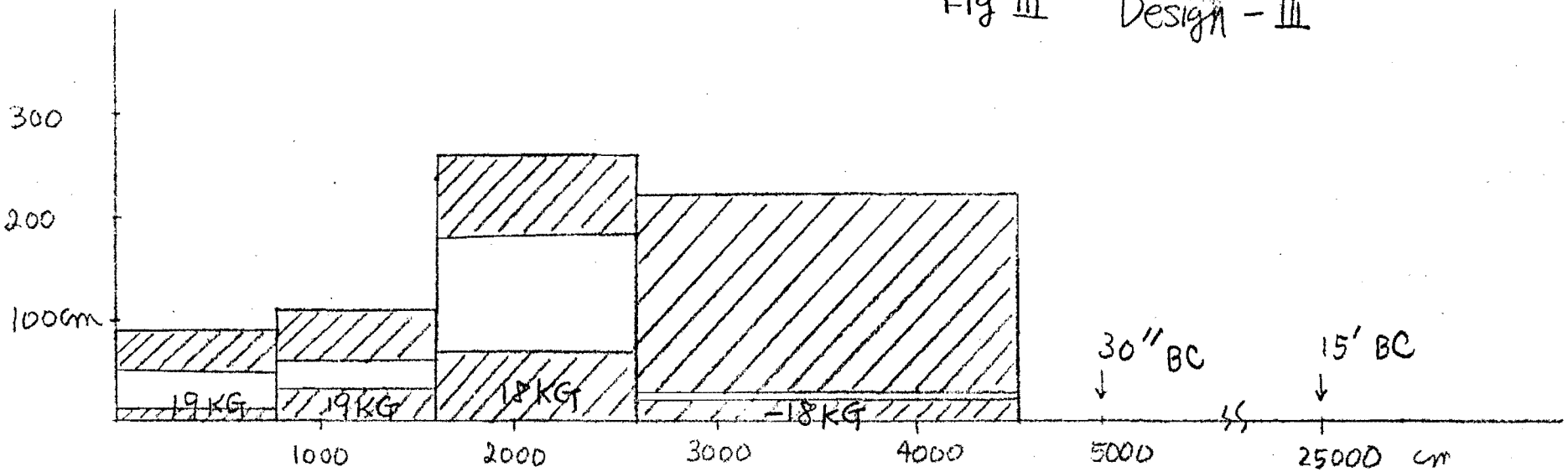

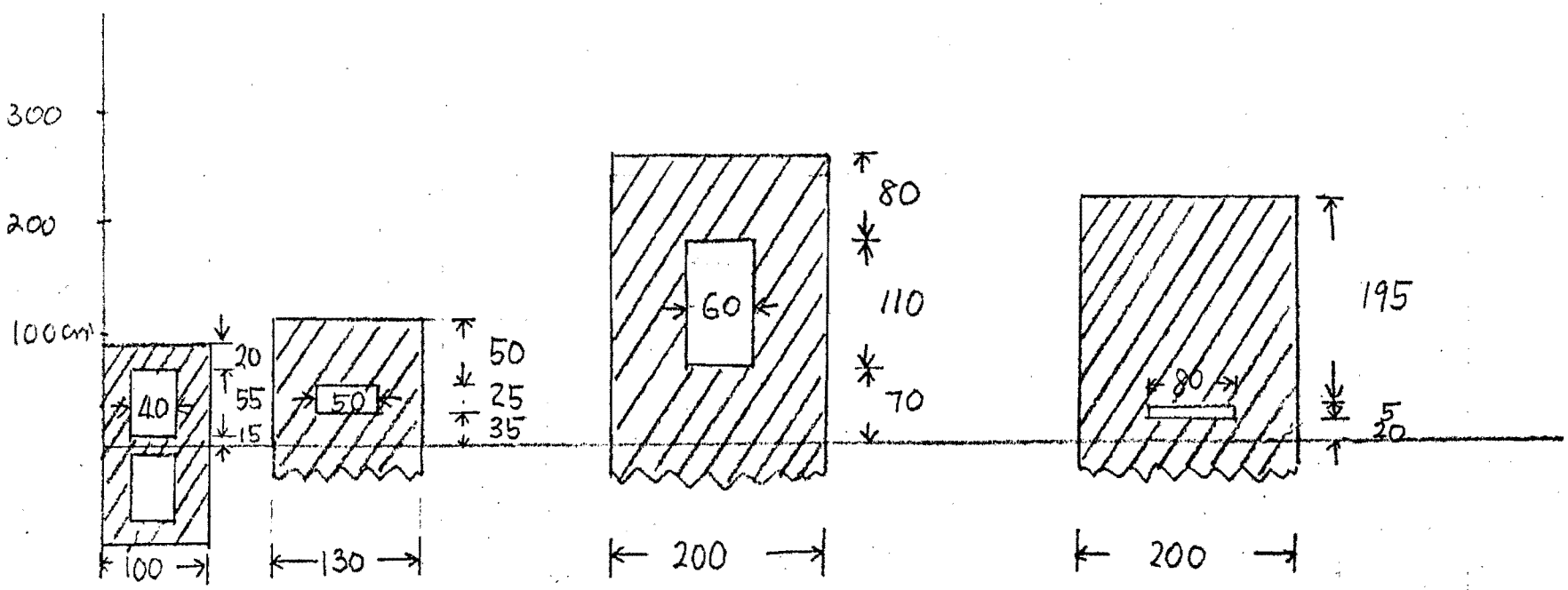

Fig IV Design IV

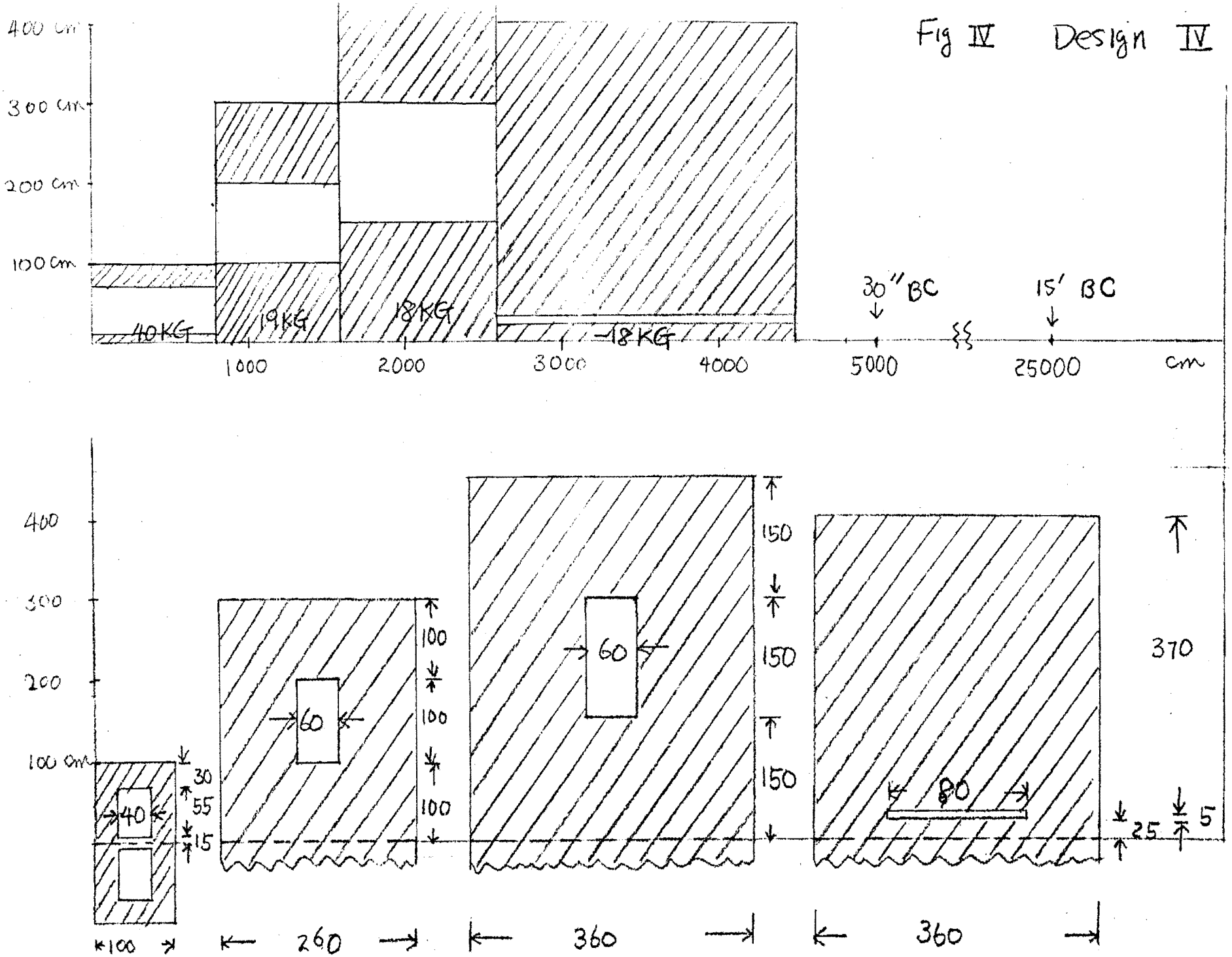

Fig V. Typical E Distribution of muons.

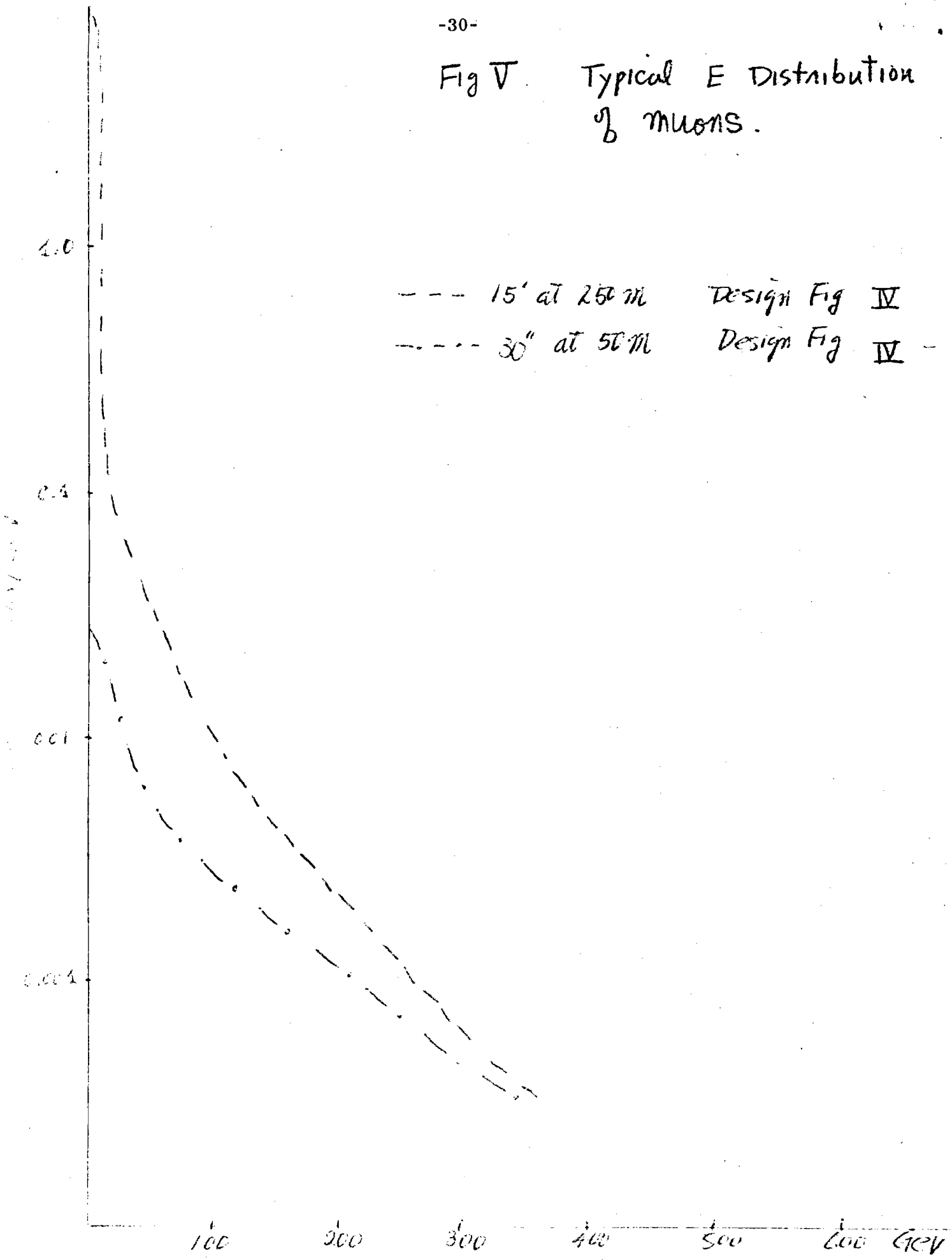

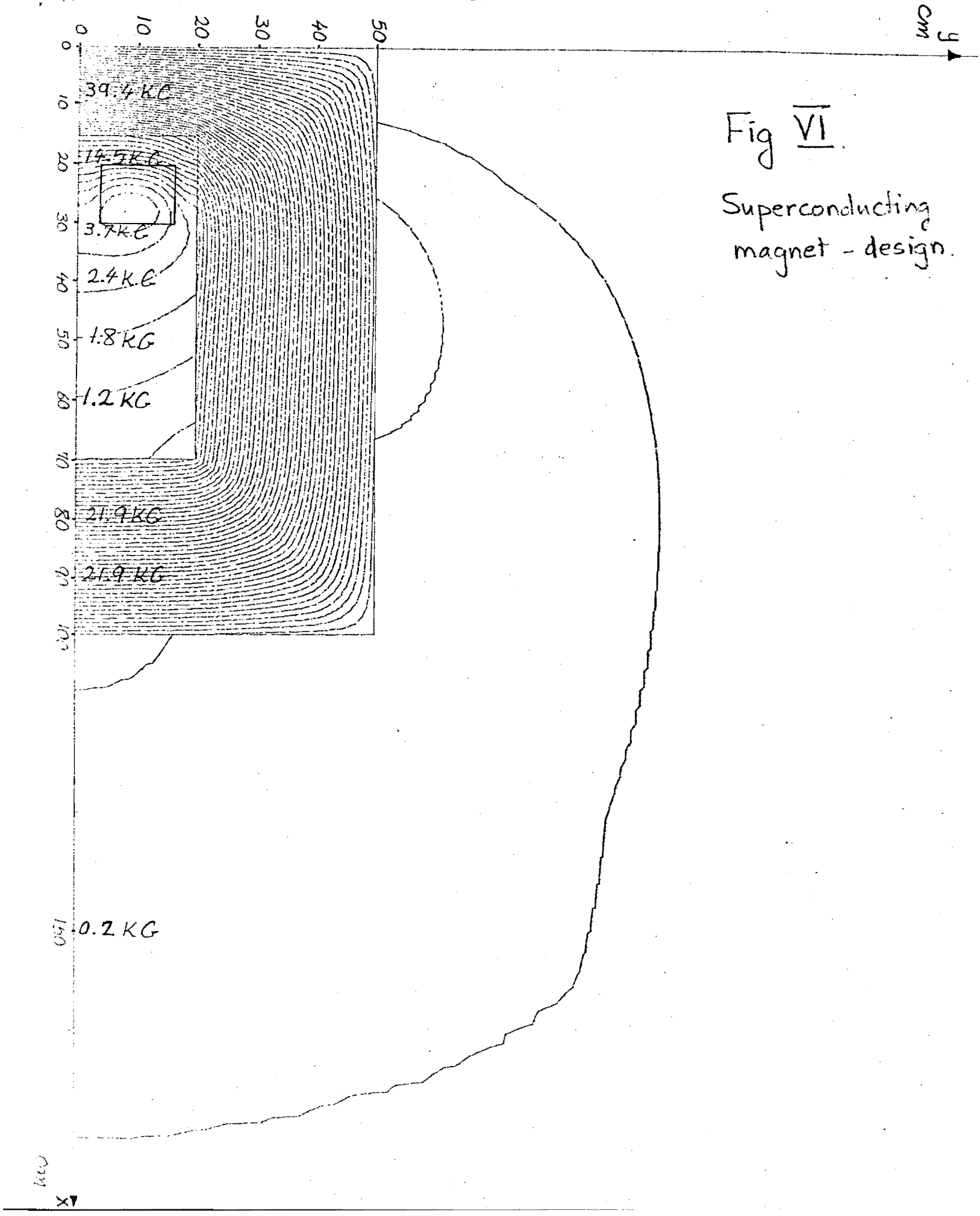

Fig VI

Superconducting magnet - design.

Table (1) - Muon Background

Design	Detector	Number of Muons entering detector/10^{13} protons			Remarks
		Algorithm I T. Kitagaki Tohoku Univ.	Algorithm II S. Oh M.I.T	Algorithm III P. HARIDAS M.I.T.	
I	15′ B.C. at 250 m	26†	7†	5†	
II	15′ B.C. at 250 m	26†	3†	3†	
	36″ B.C. at 50 m		0.5	0.5	
III	15′ B.C at 250 m	32†	40†		
	36″ B.C. at 50 m	260	100		
IV	15′ B.C at 250 m	29†*	4†	0.8†	1st magnet is super-conducting.
	36″ B.C. at 50 m	40*	1	0.5	

† A 20 GeV cut-off was applied in selecting muons entering the detector

* These values are for the geometry of design III, but with a superconducting 1st magnet. The somewhat large values here is caused by the smaller size of the magnets in design III as compared to that of IV.

Table (2) – Active Shield Weights

Design	Active shield COMPONENTS	Weight of each component	Total Weight.
I	Magnet	5360	13,400 tons
	Absorber	8040	
II	Magnet	5360	13,400 tons
	First Absorber	6250	
	Second Absorber	1790	
III	First Magnet	90	1920 tons
	Second Magnet	160	
	Third Magnet	990	
	Fourth Magnet	680	
IV	First Magnet	90	7330 tons
	Second Magnet	890	
	Third Magnet	2430	
	Fourth Magnet	3920	

Note: In addition to the above components all designs require an iron shield in front of the 15′ chamber weighing approximately 1500 tons.

Table (3) Excitation Characteristics of Superconducting Coil.

I $\times 10^6$ Ampturns	$\overline{(B_y)}_{coil}$ K Gauss	$\overline{(F_x)}_{coil}$ $\times 10^5$ N/m	$B_y(0,0)$ K Gauss	$B_y(50,0)$ K Gauss	$B_y(100,0)$ K Gauss
0·2	6·9	−1·4	31·9	−0·4	−18·8
0·3	9·3	−2·8	36·0	−1·0	−20·9
0·4	15·6	−6·2	39·3	−1·8	−21·9
0·5	17·5	−8·8	42·2	−2·7	−22·3
0·6	18·9	−11·3	45·6	−3·6	−22·8

Appendix II - Experimental Equipment

Figure 1 is a plan view of our equipment. We show upstream PWC systems and downstream PWC, Drift Chamber and CRISIS systems. These components are part of our current experiment, E565-E570. The barrel trigger hodoscope is new. This is shown in Fig. 2. This consists of two layers of 16 picket fence counters each. This allows coincidence measurement on even single tracks passing through the downstream part of the bubble chamber. The "downstream counters" would have active material only in the region of the bubble chamber volume, while the "upstream" counters would have active material extending well beyond both edges of the bubble chamber volume. The precise definition of "upstream" and "downstream" will be made only after extensive Monte Carlo studies.

The muon detector is self-explanatory, and is based on well-proven construction techniques and therefore presents no new concepts.

For particles of low momentum, our bubble chamber measurements are dominated by multiple scattering. For high momenta, the bubble chamber measurements are dominated by our setting error. The RMS sagitta caused by multiple scattering is given by

$$\delta S_{MS} = \frac{.015L}{4\ 3}\sqrt{\frac{L}{X}} = \frac{.00216}{P}\frac{L^{3/2}}{\sqrt{X_0}}$$

The sagitta due to the magnetic field is given by

$$S = \frac{.03}{8}\frac{HL^2}{P} = .00375\frac{HL^2}{P}$$

The momentum accuracy imposed by multiple scattering is given by

$$\left.\frac{\Delta P}{P}\right|_{MS} = \frac{\delta S_{MS}}{S} = \frac{.57}{H\ L\ X_0}$$

The momentum accuracy due to a setting error ΔS is given by

$$\left.\frac{\Delta P}{P}\right|_{SE} = \frac{\Delta S}{S} = \frac{.00005}{S} = \frac{.0133}{HL^2} P$$

Where all distances are in meters, P is in GeV/c and H is in kilogauss.

For our chamber $L = .5$, $X_0 = .11$, $H = 30$, hence:

$$\left.\frac{\Delta P}{P}\right|_{MS} = .08$$

$$\left.\frac{\Delta P}{P}\right|_{SE} = .0018\ P$$

Hence $\left.\frac{\Delta P}{P}\right|_{MS} = \left.\frac{\Delta P}{P}\right|_{SE}$ At about 30 GeV/c. The use of our downstream spectrometer will reduce our errors to:

$$\frac{\Delta P}{P} \cong .0006\ P$$

Since typical freons (see table) have radiation lengths of about 11 centimeters our chamber is an excellent gamma ray detector. The average gamma ray will see about 4.5 radiation lengths and hence will have over a 95% probability of conversion. Hence we should be able to detect most gamma rays and measure their momentum to better than 25% for gamma rays with energies less than 30 GeV/c.

The chamber is also an excellent electron detector, as there is again an over 95% probability that an electron will shower before leaving the chamber.

APPENDIX II - FIG. 1

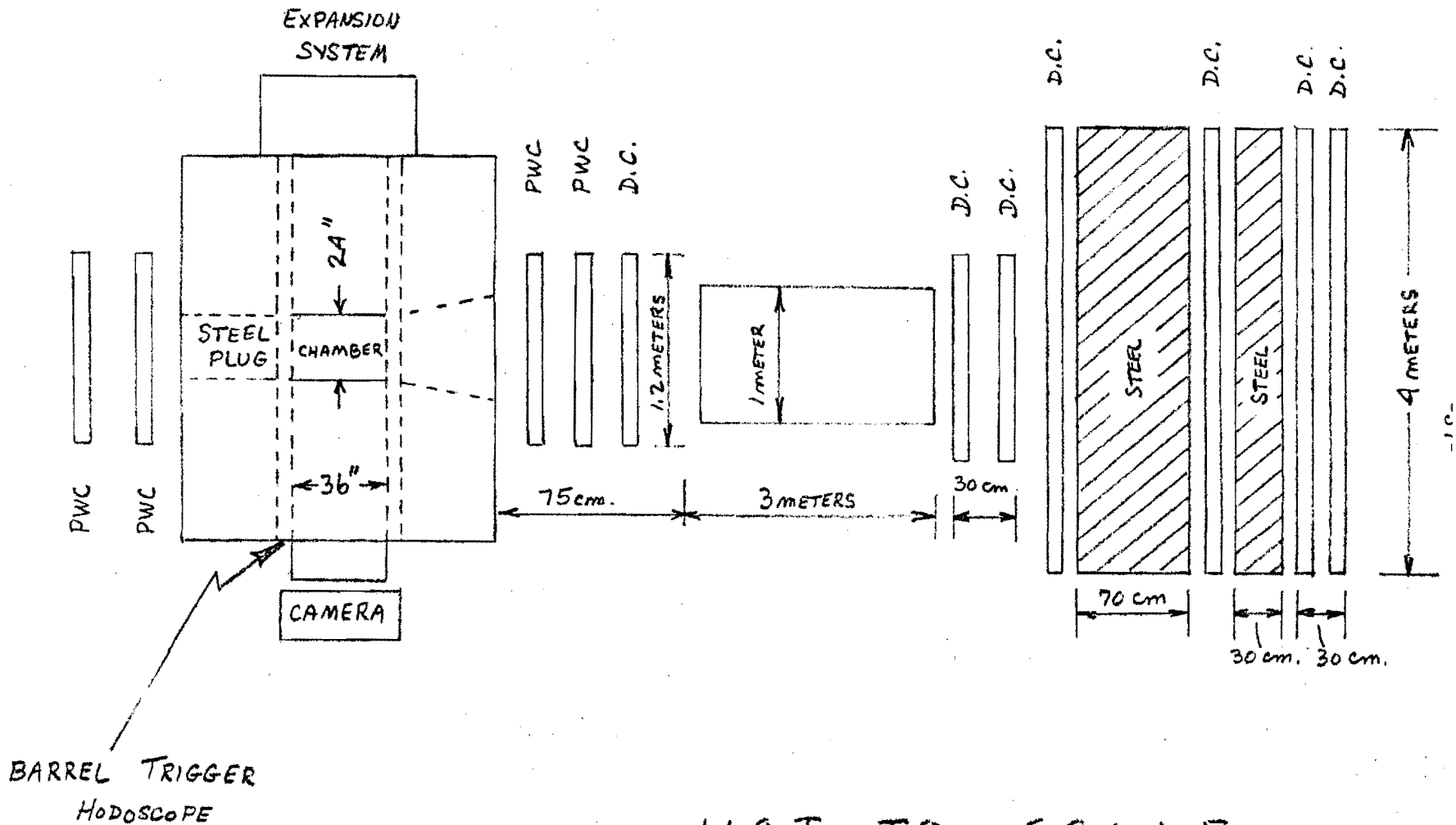

NOT TO SCALE

Appendix II - Fig. 2

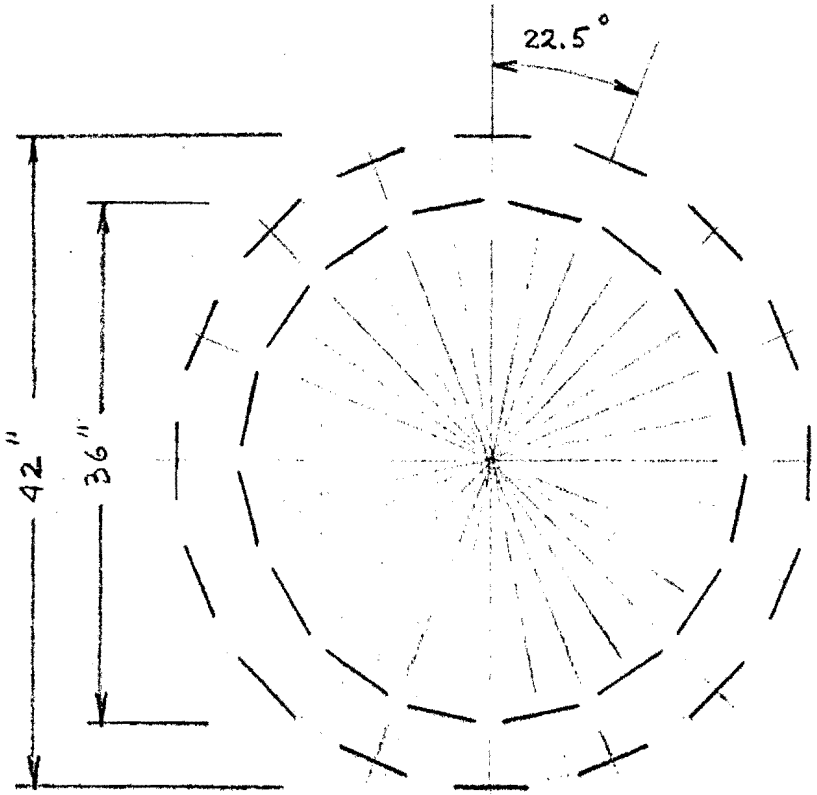

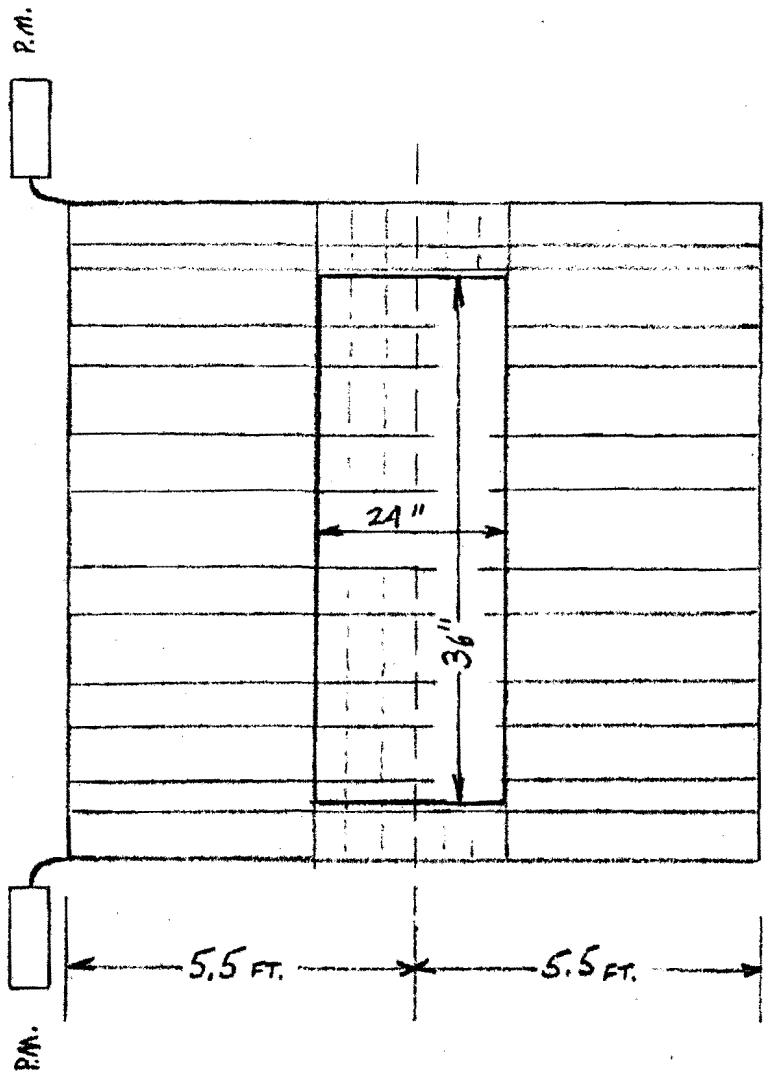

APPENDIX II

TABLE II
PRINCIPAL CHARACTERISTICS OF LIQUIDS USED

Liquids	Density ρ (gm/cm^3)	Radiation length X_0 (cm)	Proportion of reactions on hydrogen	Mean interaction length (cm) assuming $\sigma_{(mb)} = 45\,A^{2/3}$	Operating temperature T (°C)	Vapor pressure P (atm)	Laboratories that have used these liquids
Propane C_3H_8	0.43	110	34%	154	58	19	Many laboratories
Xenon Xe	2.3	3.9	0	80	−19	26	Ann Arbor, Berkeley, Dubna
Freon CF_2Cl_2	1.12	21.5	0	97	70	18	CERN
Freon CF_3Br	1.50	11	0	82	30	18	École Polytech., CERN
Freon C_2F_5Cl	1.20	25	0	83	40	14	École Polytech.
$C_3H_8 + CF_3Br$ 86% 14%	0.56	52	29%	137	49	18.5	École Polytech.
$C_3H_8 + CF_3Br$ 50% 50%	0.91	22	17%	107	37	18	École Polytech., Berkeley
$C_2F_5Cl + CF_3Br$ 50% 50%	1.35	17	0	82.5	36	16	École Polytech.
$C_3H_8 + CH_3I + C_2H_6$ 33% 33% 33%	1.05	11.4	23%	107	28	31	M.I.T., Harvard

Appendix III - Event Rates

Taking the neutrino fluxes calculated by S. Mori, we have corrected for the linear dependence on energy of the neutrino-nucleon cross section. The results are shown in Fig. 1, where each curve represents average over 2mrad. wide radial bins.

Figure 2 shows the result of integrating these fluxes over the entire energy range. The solid points correspond to the curves in Fig. 1, while open points correspond to curves at intermediate angle ranges as formed by interpolation. The abscissa, R, is the effective radius of a detector at distance D from the beam dump.

The 15' chamber at D = 250 meters and our detector at D = 50 meters are located on the graph for comparison. Integrating over R and accounting for the differences in depth and density of the two chambers gives an expected 3300 events for the 15' as compared to 2200 for our detector.

Fermilab

April 3, 1980

TO: BEAM DUMP ENTHUSIASTS

FROM: J.K.WALKER JKW

SUBJECT: NEUTRINO FLUX

After some discussions, we have settled on the fluxes in the two attached figures. We have investigated the technology and cost of pure tungsten material for a dump and find it acceptable. Compared to copper the tungsten is attractive for two reasons. The cross sections for D and F are assumed to scale as atomic weight (we use σ_D = 34 μb at 1 TeV). The other reason is less non-prompt neutrinos. The resulting ν_e flux is four times that given originally by S.Mori and is shown in the figure for different detector distances. The factor of four comes about from two factors of two -- one for A dependence and one for energy dependence of the D cross section.

For ν_τ flux we assume that $\frac{\sigma(F)}{\sigma(D)} = 0.25$ rather than 0.1 which was assumed by S.Mori. The resulting ν_τ flux is a factor of ten higher than that given originally by S.Mori. The ν_τ flux is shown for various detector distances in the attached graph.

The T.M. is being typed now and can be referred to as TM-953 by S.Mori and J.K.Walker. The title is "A Flavored Neutrino Beams Facility". As soon as it is available, I will send you a copy.

JKW:lls
Attchs. (2)
cc C.Baltay - CERN
M.Peters - Hawaii
V.Peterson - Hawaii
W.Busza - MIT
R.Fine - Columbia
H.Bingham - LBL
I.Pless - MIT
D.Garelick - North Eastern

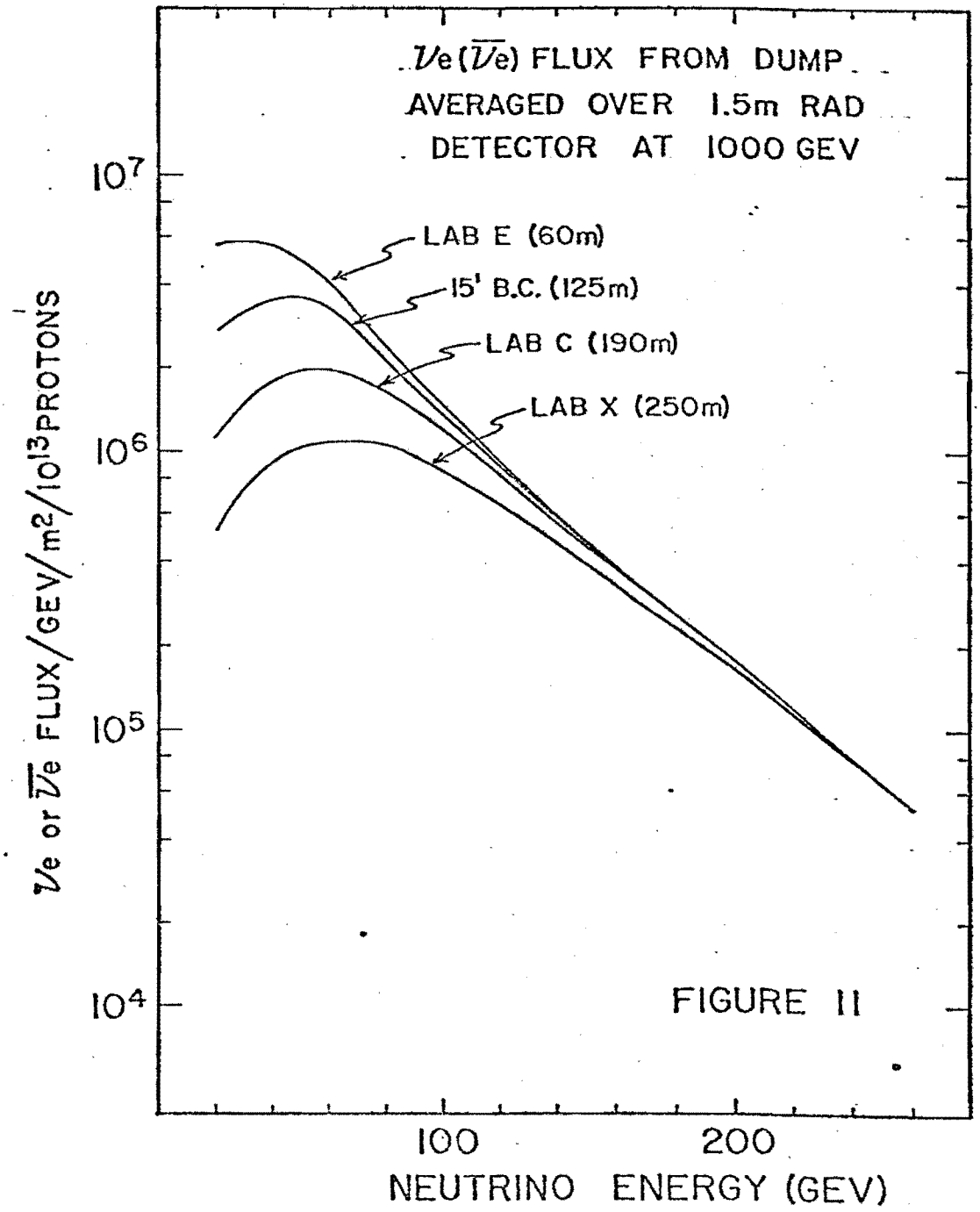
$\nu_e(\bar{\nu}_e)$ FLUX FROM DUMP
AVERAGED OVER 1.5m RAD
DETECTOR AT 1000 GEV
LAB E (60m)
15' B.C. (125m)
LAB C (190m)
LAB X (250m)
10^7
10^6
10^5
10^4
ν_e or $\bar{\nu}_e$ FLUX/GEV/m^2/10^{13}PROTONS
100
200
NEUTRINO ENERGY (GEV)

FIGURE 11

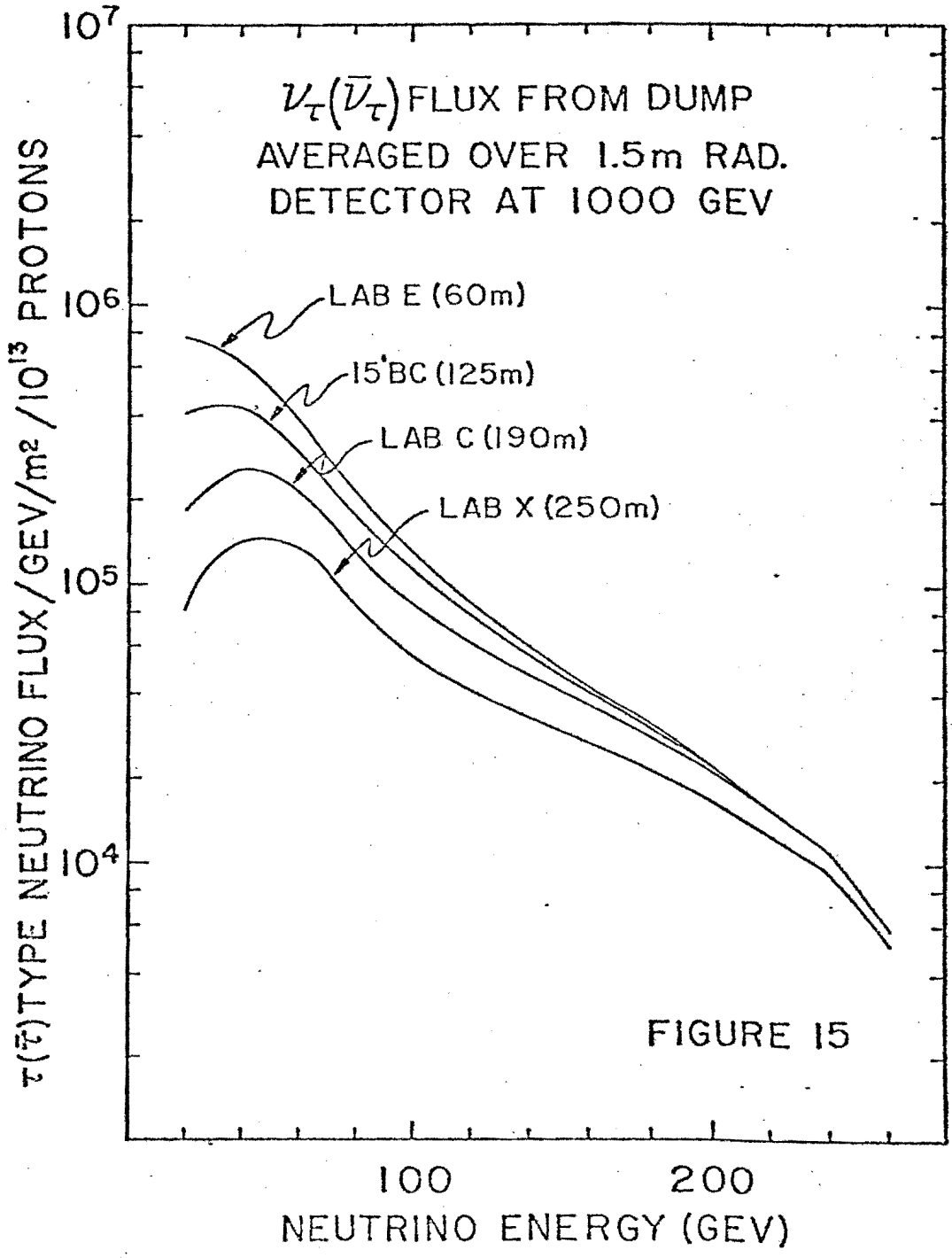
$\nu_\tau(\bar{\nu}_\tau)$ FLUX FROM DUMP
AVERAGED OVER 1.5m RAD.
DETECTOR AT 1000 GEV
LAB E (60m)
15°BC (125m)
LAB C (190m)
LAB X (250m)
10^7
10^6
10^5
10^4
$\tau(\bar{\tau})$ TYPE NEUTRINO FLUX/GEV/m² /10^{13} PROTONS
100
200
NEUTRINO ENERGY (GEV)

FIGURE 15

APPENDIX III - FIG. 1

ENERGY WEIGHTED FLUX AT 250 METERS

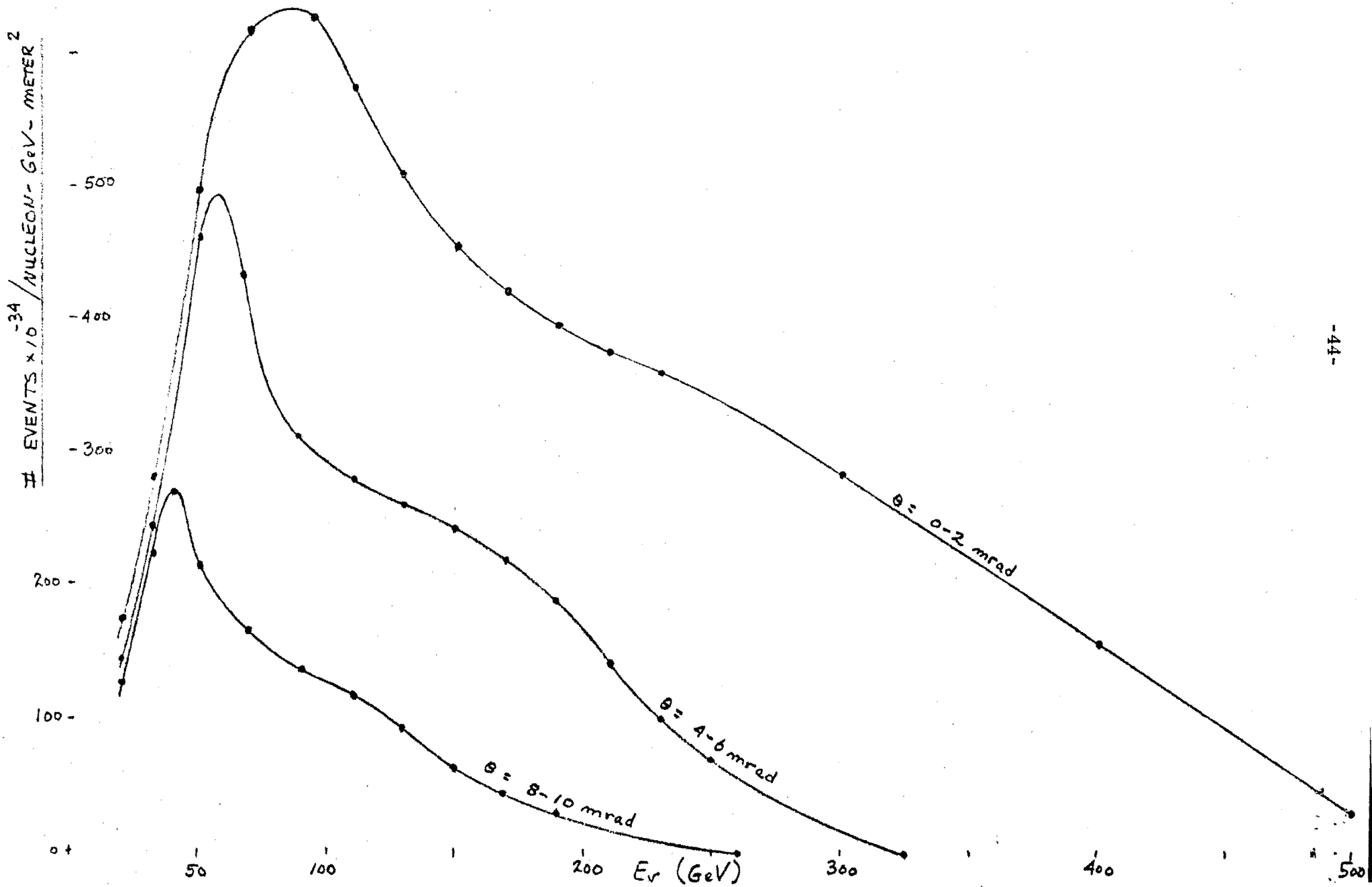

APPENDIX III - FIG 2

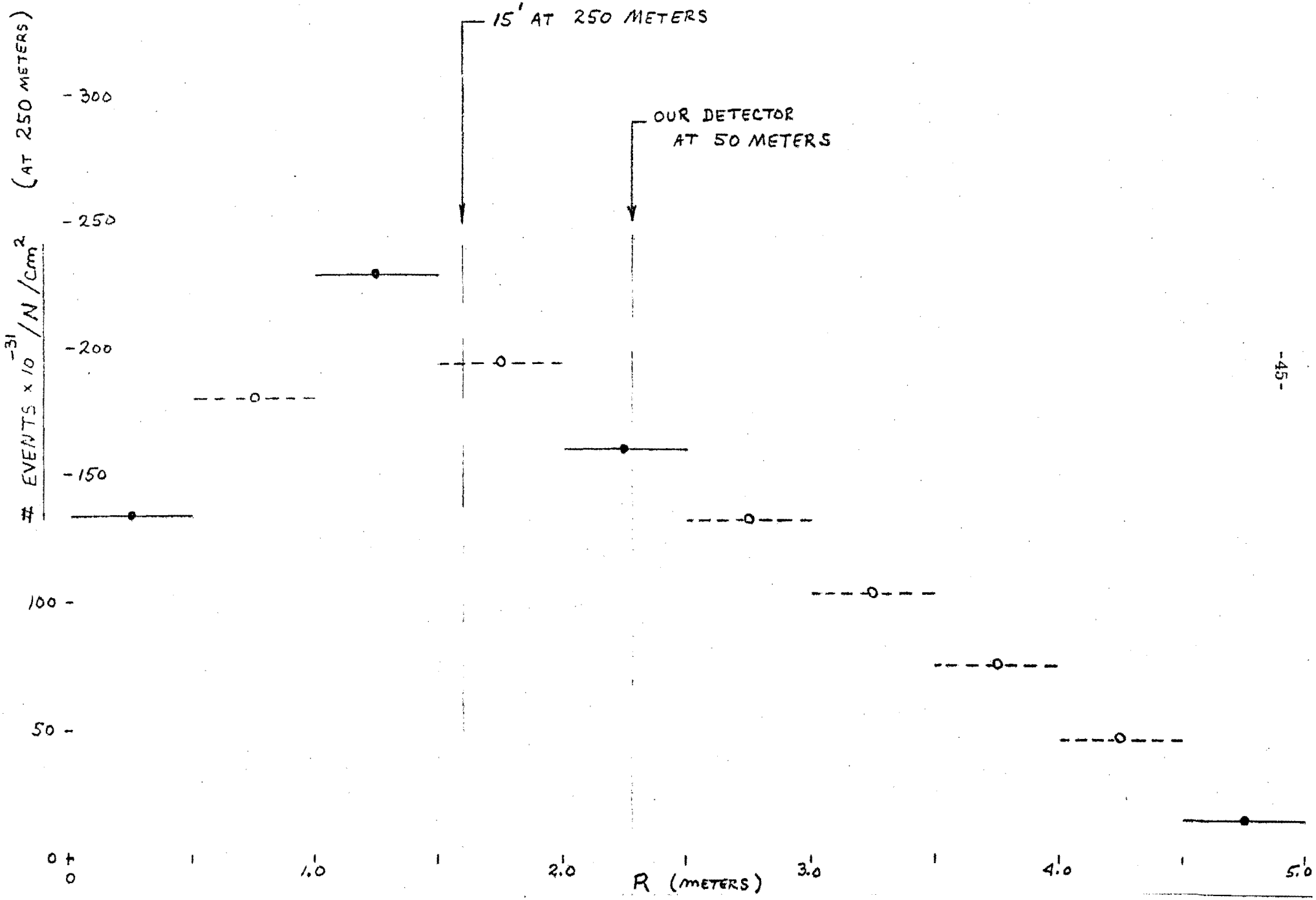

Based on the ν_τ flux distribution at 1000 GeV (S. Mori) we have simulated ν_τ events for the bubble chamber reactions:

$$\bar{\nu}_\tau + N \rightarrow \tau^+ + \text{hadrons}$$

$$\nu_\tau + N \rightarrow \tau^- + \text{hadrons}$$

Assuming the X and Y distributions:

$$\left.\begin{array}{ll} \nu_\tau \text{ events:} & Y \text{ FLAT} \\ \bar{\nu}_\tau \text{ events:} & (1-Y)^2 \end{array}\right\} \cdot X^{0.2} (1-X)^{3.5}$$

and the relation between cross sections:

$$\frac{\sigma_{cc} (\bar{\nu}_\tau)}{\sigma_{cc} \nu_\tau} = 0.378$$

the resulting τ energy distribution in the lab (for τ^+, τ^- combined) is shown in fig. 1a. For the comparison we have also simulated such events by using the experimentally measured ν_μ flux distributions, but assuming γ's were produced. Figure 1b shows the energy distribution for this case.

We next assume the expected τ lifetime: $\tau_\tau = 2.8 \times 10^{-13}$ sec. and have determined the decay lengths for these simulated events, accounting only for the leptonic decays:

$$\tau^- \rightarrow e^- \bar{\nu}_e \nu_\tau \qquad (\tau^+ \rightarrow e^+ \nu_e \bar{\nu}_\tau)$$

$$\tau^- \rightarrow \mu^- \bar{\nu}_\mu \nu_\tau \qquad (\tau^+ \rightarrow \mu^+ \nu_\mu \bar{\nu}_\tau)$$

for which the rate is calculated to be given by:

$$\frac{d\Gamma}{dZ\, d\cos\theta} = \frac{1}{\tau_\tau} Z^2 \left[(3-2Z) + a \cos\theta\, (1-2Z) \right]$$

where: $Z = \dfrac{2E_\ell}{M_\tau}$

E_ℓ = Energy of the produced lepton

$$a = \begin{cases} +\beta \text{ for } \tau^+ \\ -\beta \text{ for } \tau^- \end{cases}$$

The differences in τ momenta are incorporated into the decay length, and the resulting distribution is shown in Fig. 2a.

Our limitation on resolving short decay length as well as small decay angle can be estimated in the following way. Given the length L between the production vertex and decay vertex, and a decay angle θ, a useful quantity which reflects both of these is the impact parameter $B = L \sin \theta$:

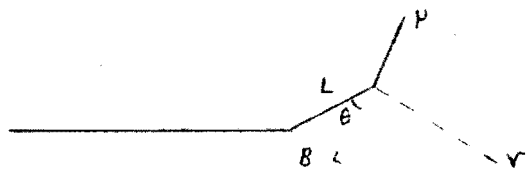

Assuming a bubble diameter of 10μ on film and a magnification of M = 12, we can determine the accuracy to which B can be measured.

We further assert that the true uncertainty is actually a factor of 5 better than this, giving:

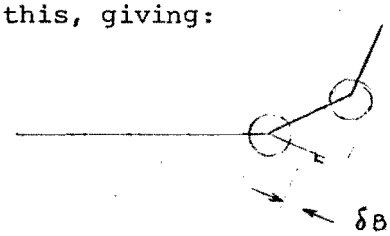

$$\delta B = 0.002 \times \sqrt{2} \times M \quad \text{mm}$$

We then require $\delta B < B/2$ or $\frac{B}{\delta B} > 2$ as our criterion for successfully measuring the event. Figure 25 gives a histogram of $B/\delta B$ showing that over 42% of the simulated events have $B/\delta B > 2$ and can therefore presumably be measured.

Expecting that we fail to measure the τ decays having $B/\delta B < 2$ it appears at first that our ability to estimate the number of τ mesons produced in our chamber and the τ meson lifetime is hampered. However, we bring to light a promising technique in the following demonstration. We again make use of the simulated events. An initial Monte Carlo run of N_0 events using the expected lifetime $\tau_\tau = 2.8 \times 10^{-13}$ sec. yields a τ decay length distribution which is dubbed as a reference, R. Subsequent runs made

with different lifetimes τ, but again with N_0 events, are treated as representing the data, D. By imposing the cut $B/\delta B > 2$ we expect to be able to extract the initial number, N_0, of ν_τ from the resulting decay length distribution. We assert that N_0 may be determined fairly accurately along with the lifetime τ by minimizing the expression:

$$\chi^2 = \sum_i \frac{(R_i - ND_i)^2}{R_i}$$

with respect to both N and τ.

We will not know the τ meson distribution in our chamber. However, we will know the μ and e distribution in our chamber. We have performed the above χ^2 minimization for both distributions.

Figures (3a, 3b) illustrate how χ^2 tends smaller as $\tau \to \tau_\tau$ and $N \to N_0$ for the simulated data originating from both the ν_τ flux distribution (Fig. 3a) and the ν_μ flux distribution (Fig. 3b). This simple χ^2 test shows promise and it is expected that more reliable methods such as the Kolmogorov test will further improve accuracy.

The above leptonic processes account for 34% of the τ decays. The two-body semileptonic decay modes ($\tau \to \pi \nu_\tau$, $\tau \to \rho \nu_\tau$, $\tau \to A_1 \nu_\tau$) represent a further 42% of the τ decays. A heavy liquid bubble chamber is well suited to detecting $\pi^0 \to \gamma\gamma$ and hence the resonant decay of the ρ and A_1. We have investigated a technique which will allow the use of these semileptonic decay events in the determination of the τ lifetime.

In the reaction

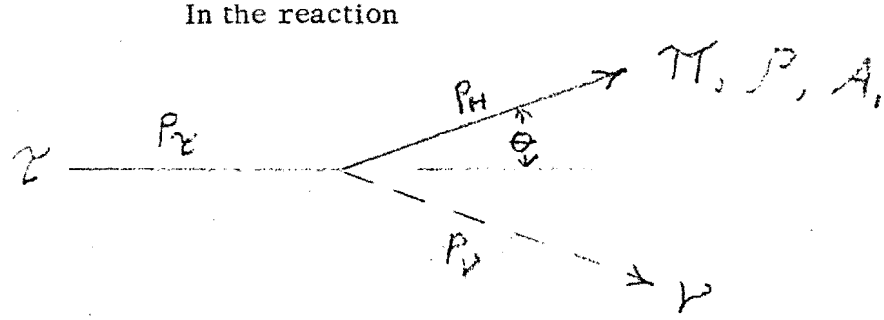

we measure P_H, the hadron momentum and production angle. Simple kinematics tells us that P_τ occurs quadratically in a relationship involving itself, measured quantities, and known particle masses. Hence, for any given event we can generate two momenta (P+ and P-), one of which is the τ momentum which in fact produced the event.

The formula for P+ and P- is:

$$P(+-) = \frac{P_H(M_\tau^2 + M_H^2)\cos\theta \pm \sqrt{P_H^2(M_\tau^4 + M_H^4 + M_\tau^2 M_H^2 \cos 2\theta) - 4M_\tau^2 P_H^2 (P_H^2 \sin^2\theta + M_H^2) + M_H^2 (M_\tau^2 - M_H^2)^2}}{2(M_H^2 + P_H^2 \sin^2\theta)}$$

A Monte Carlo provides an idea of how P+ and P- reflect P_τ as we generate P+ and P- from a known P_τ.

A Monte Carlo as described above was performed, the only modification being the two-body decay of the tau (with an angular dependence 1- a $\cos\theta$). We used the pion mass and further put typical bubble chamber measurement errors on P_H before calculating P+ and P-. We find that half of the time P+ is correct and likewise for P-. For each P+ and P-, we calculate the proper decay time in the Monte Carlo and histogram both points. If P+ is wrong, we expect it contributes too short a lifetime, while P- gives too long a lifetime when it is wrong. We therefore expect a middle range of proper decay times to yield the correct τ lifetime.

First we check our Monte Carlo (Fig. 4) in τ lifetimes (τ_τ) and find good results (arrows indicate the range of points fitted over in all plots). Next we impose the cut $B/\delta B \geq 2$ (Fig. 5) and find too small a lifetime. This is expected as the sample after the cut contains relatively longer laboratory decay times, hence high momentum and

short proper time. Note that this distribution and the above derive from P_τ chosen by the Monte Carlo. Finally, we calculate P+ and P- from P_H generated by Monte Carlo with experimental errors and histogram (Fig. 6). We restrict the range of the fit as mentioned earlier and find a lifetime of 0.76 τ_τ . We expect, however, to correct this by at least the losses show in making the necessary B/δB cut indicating a lifetime of 0.83 τ_τ - a measurement 17% too low. Hence we can use the two-body decay modes to make a reasonably accurate measurement which we can compare to the technique described earlier which uses only track length distributions.

APPENDIX IV

FIG 1a

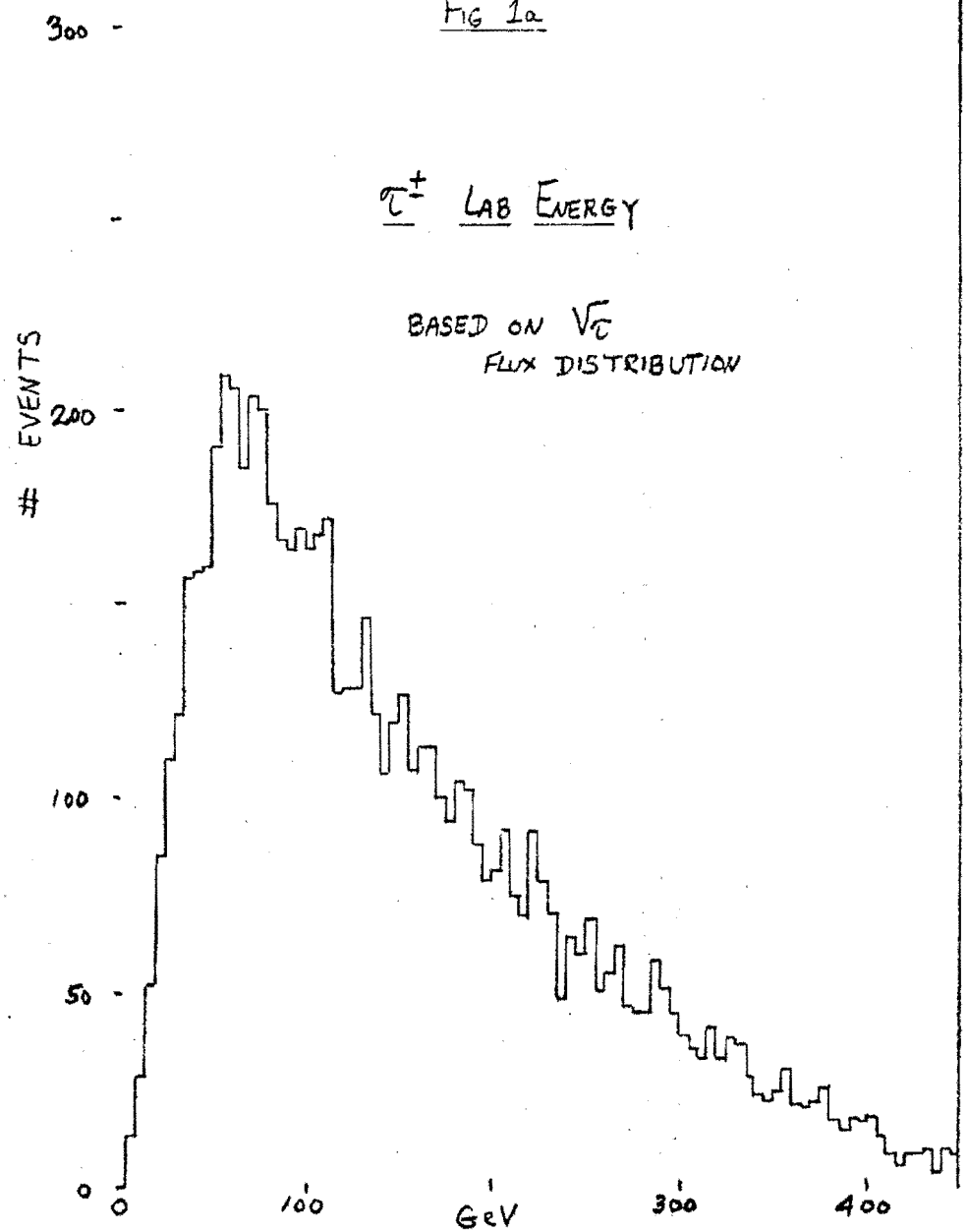

APPENDIX IV

FIG. 1b

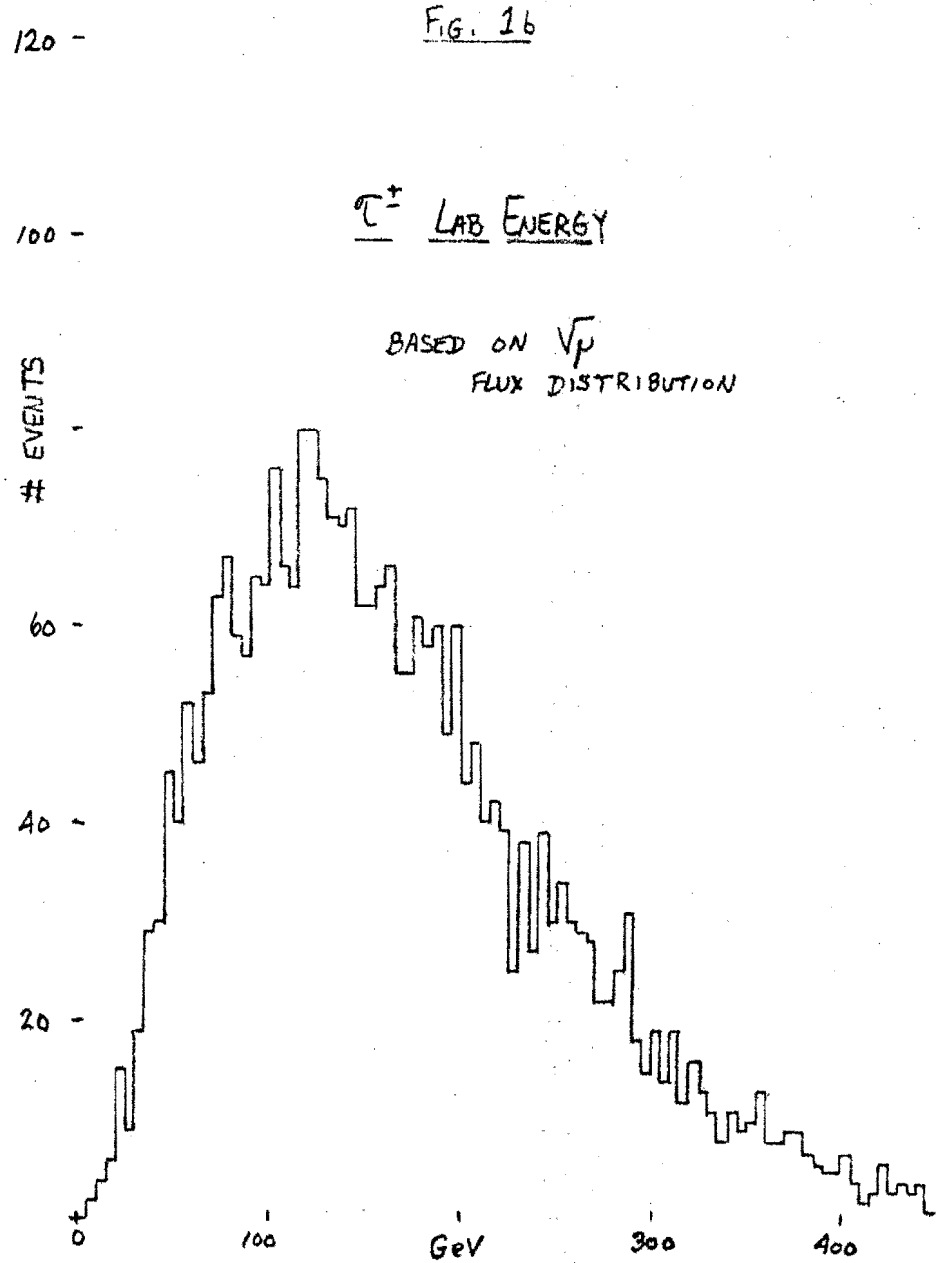

APPENDIX IV

FIG. 2a

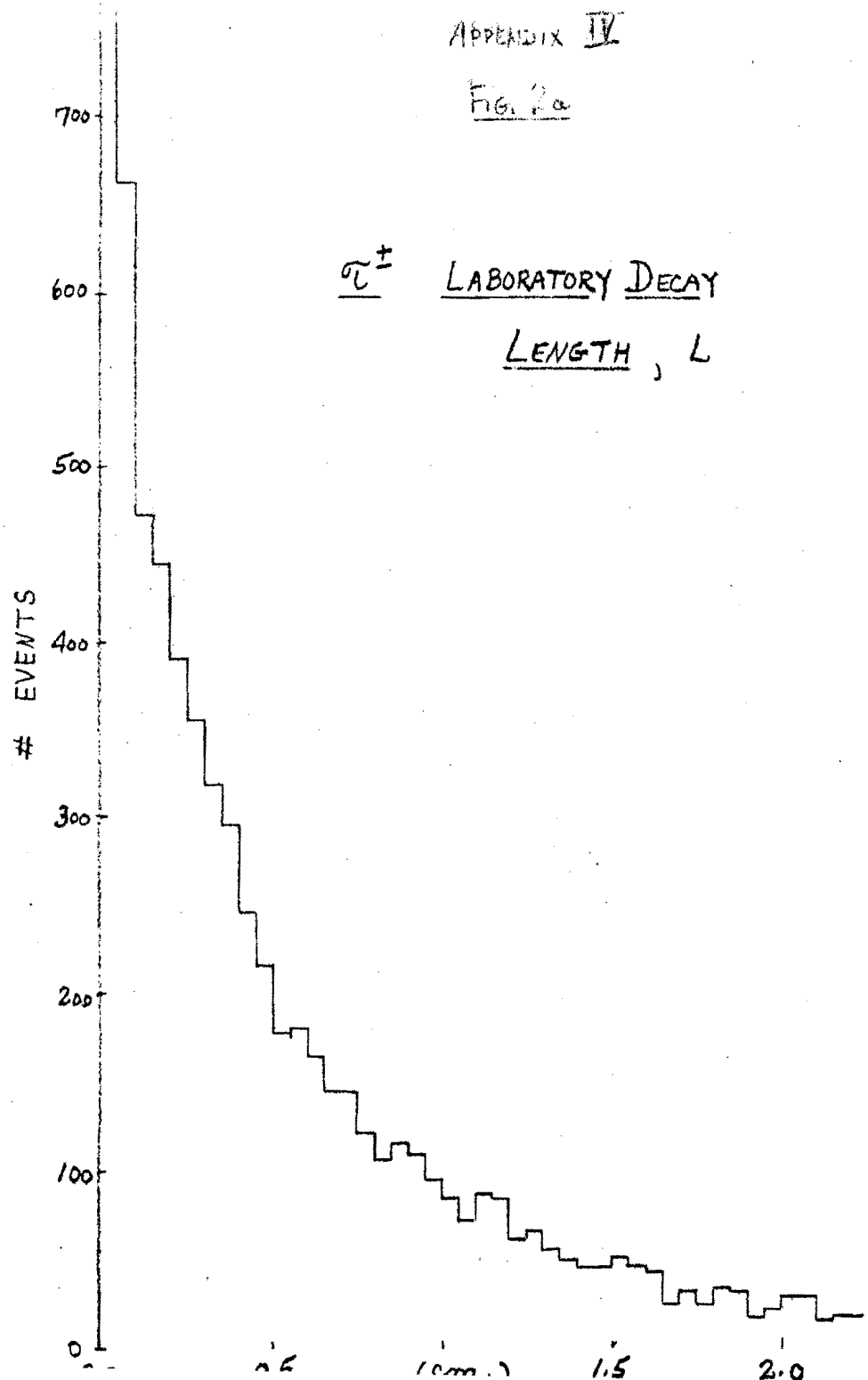

APPENDIX V

FIG. 2b

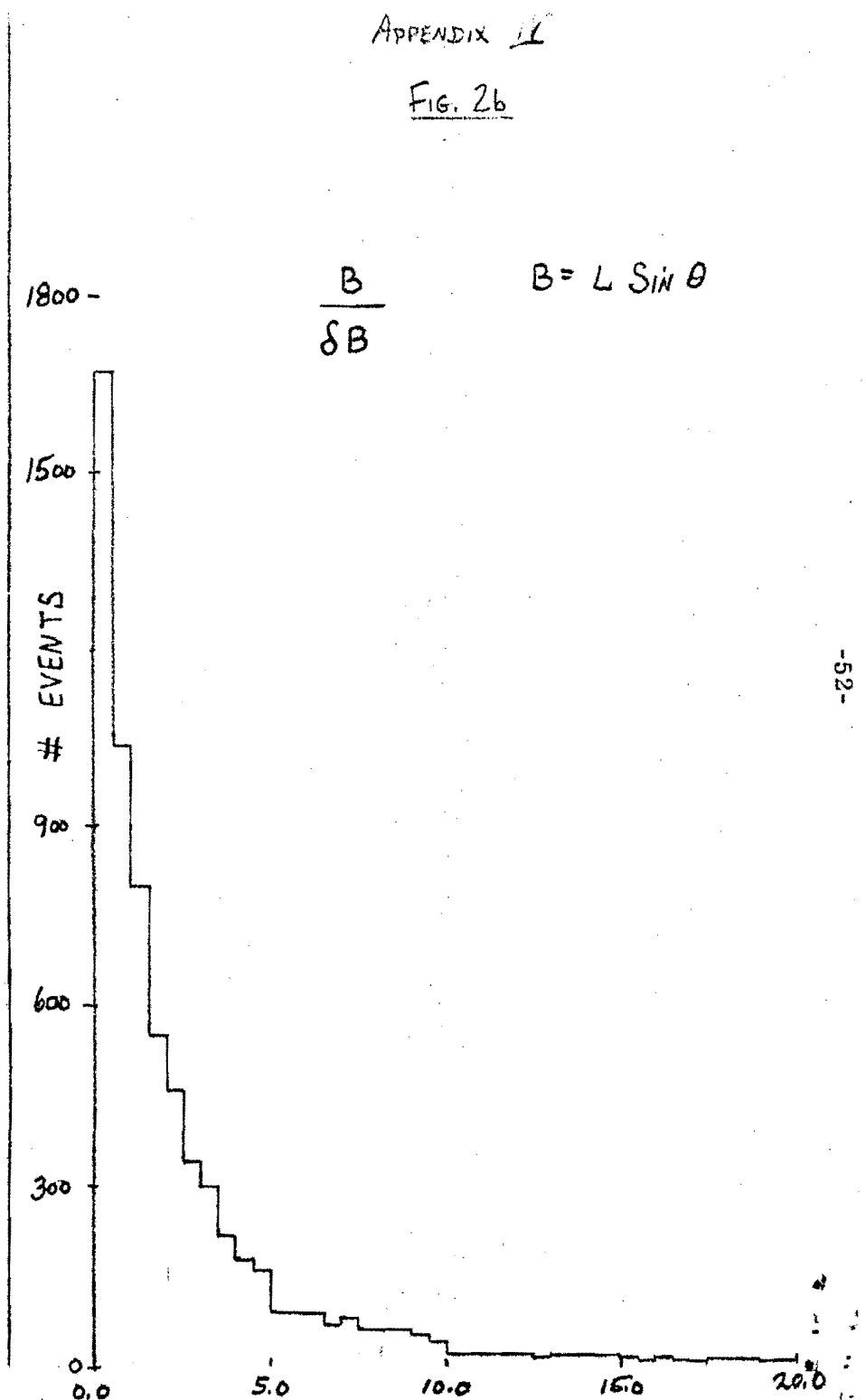

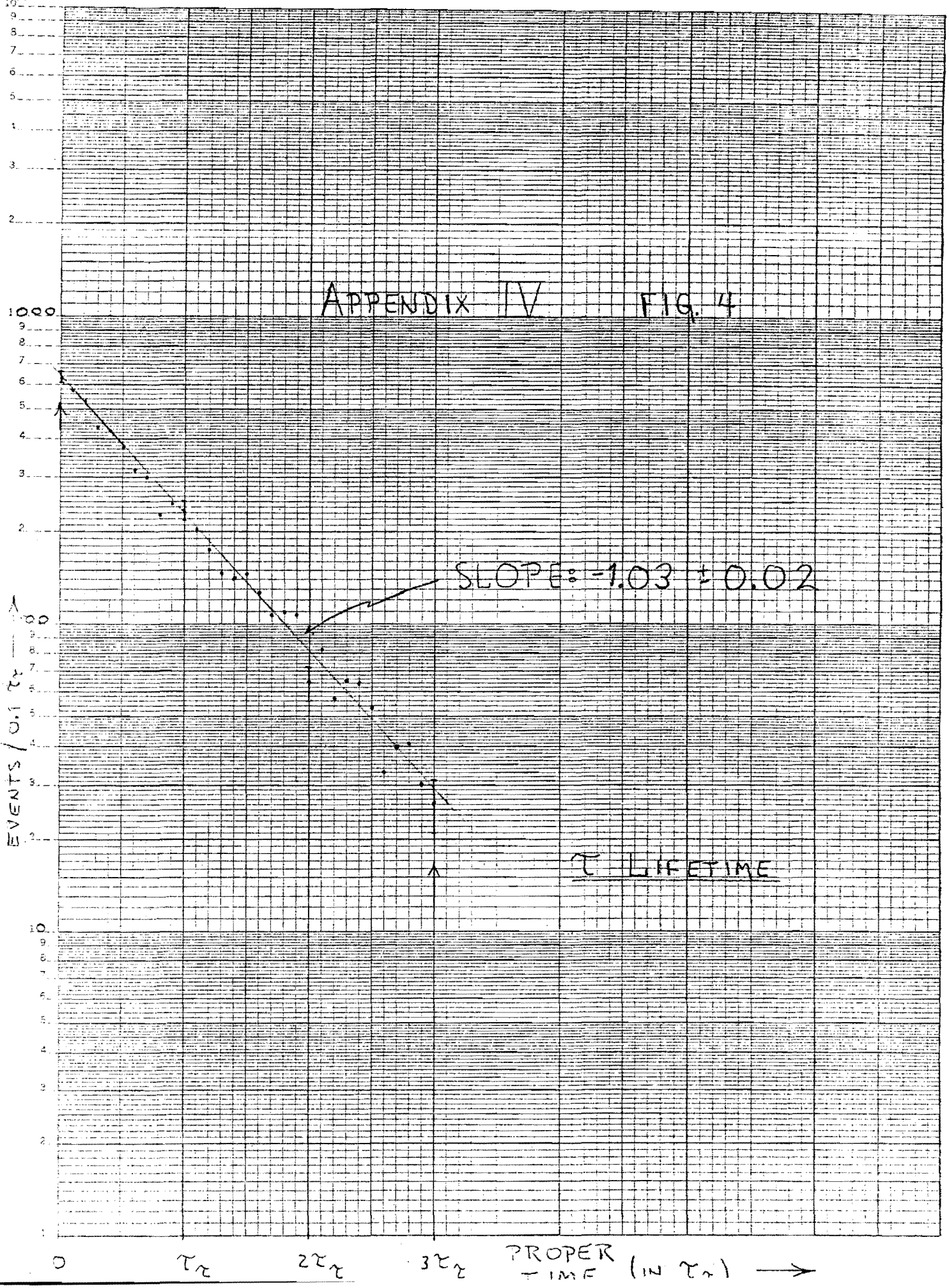
APPENDIX IV FIG. 4
SLOPE: -1.03 ± 0.02
τ LIFETIME
EVENTS / 0.1 τ_τ
0
τ_τ
2τ_τ
3τ_τ
PROPER TIME (IN τ_τ)

APPENDIX IV
FIG 3a

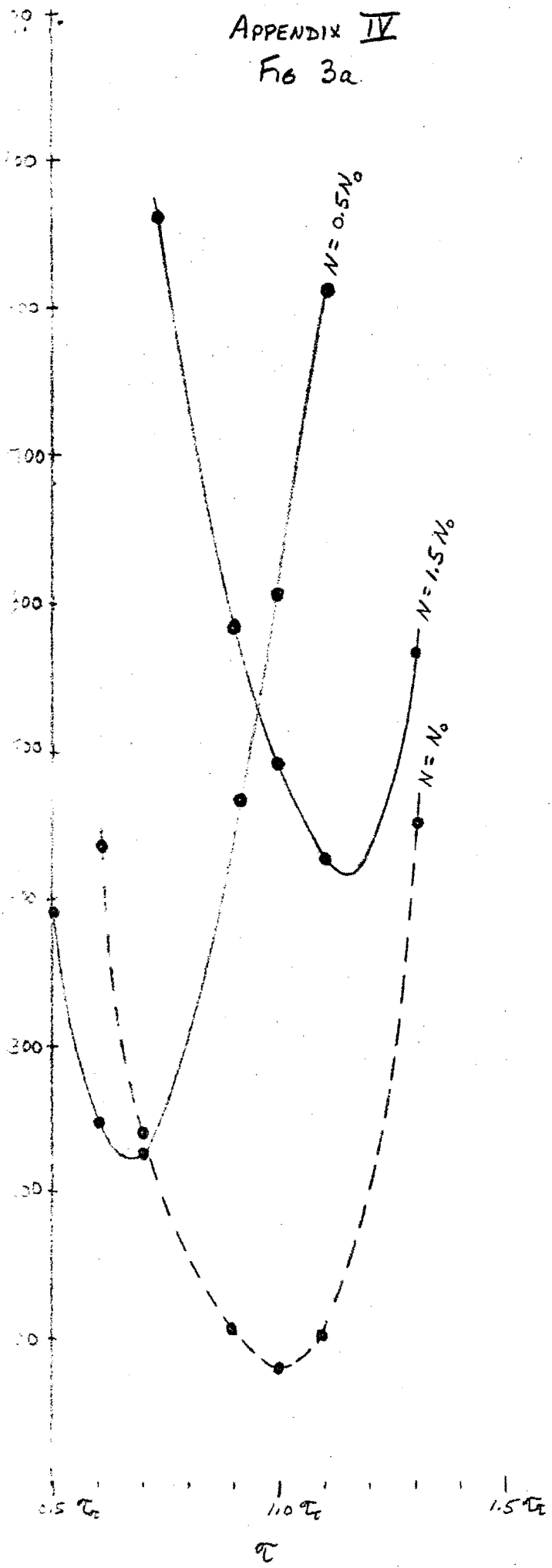

APPENDIX IV
FIG 3b

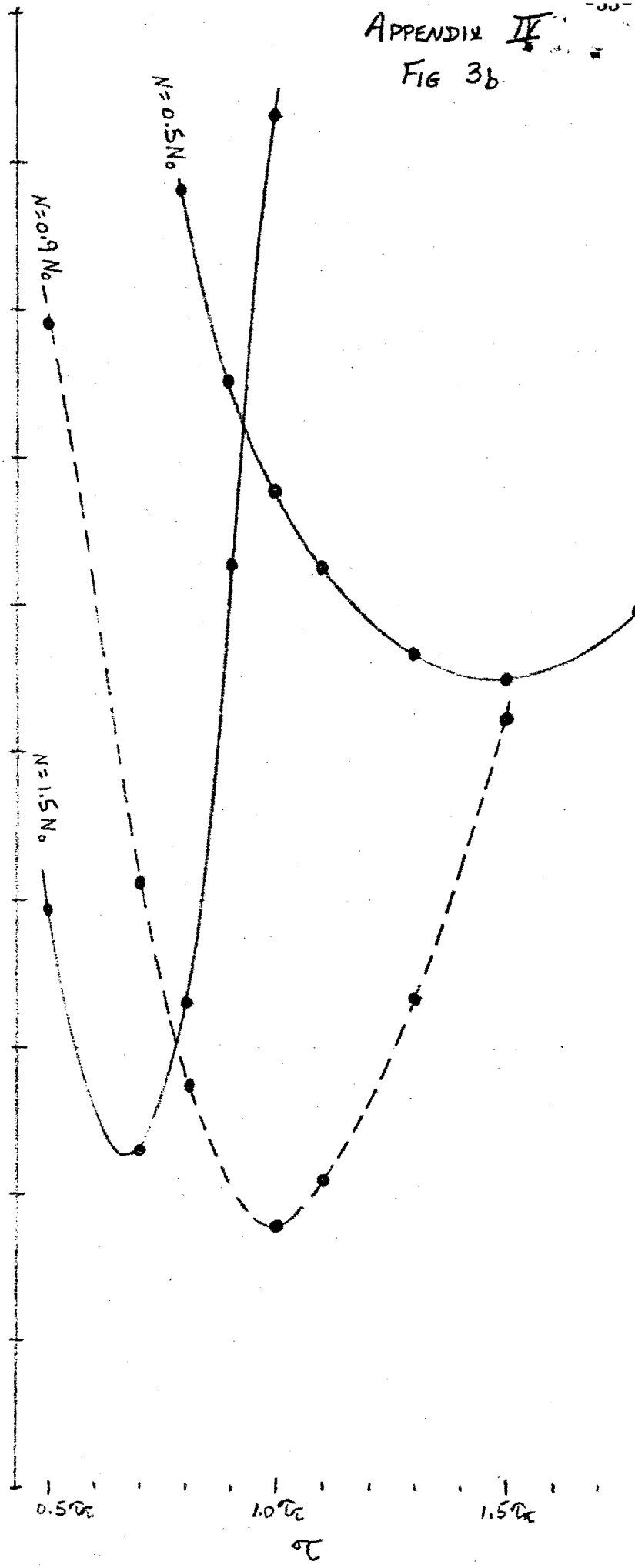

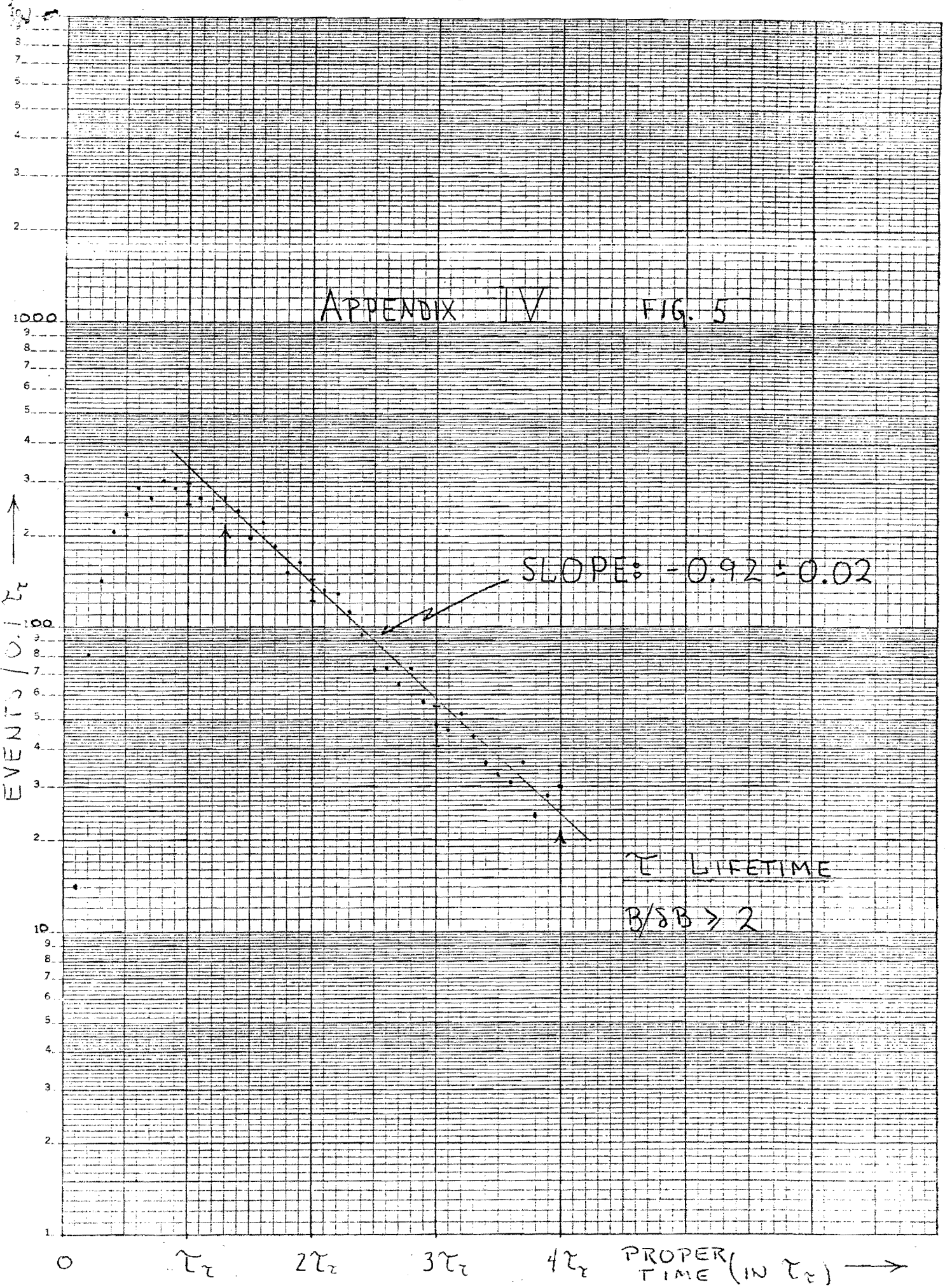
APPENDIX IV
FIG. 5
SLOPE: -0.92 ± 0.02
τ LIFETIME
B/δB ≥ 2
EVENTS / 0.1 τ_τ
0
τ_τ
2τ_τ
3τ_τ
4τ_τ
PROPER TIME (IN τ_τ)

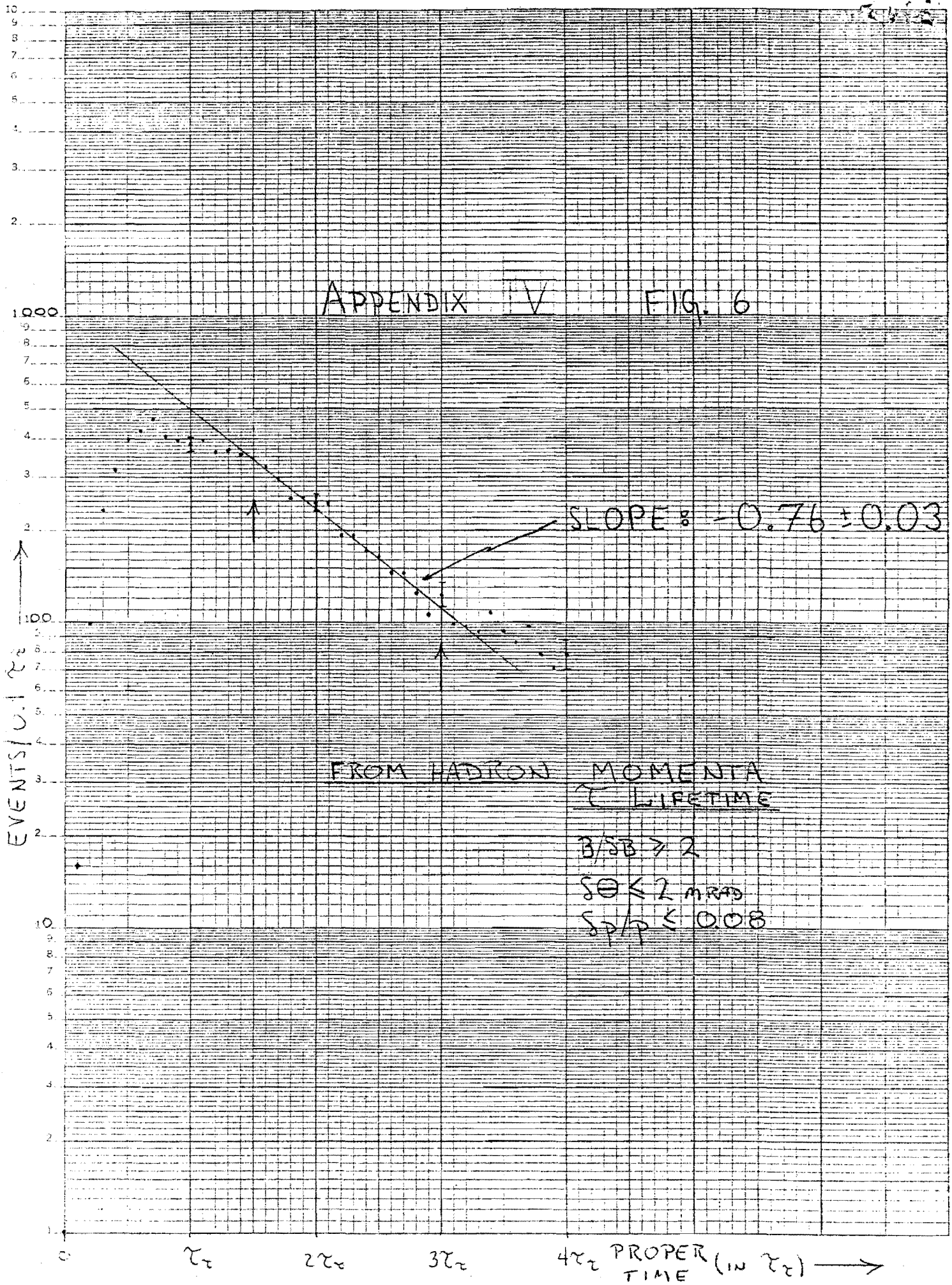
APPENDIX V FIG. 6
SLOPE: -0.76 ± 0.03
EVENTS/0.1 τ_τ
FROM HADRON MOMENTA
τ LIFETIME
$B/\delta B \geq 2$
$\delta\theta \leq 2$ mrad
$\delta p/p \leq 0.08$
τ_τ
$2\tau_\tau$
$3\tau_\tau$
$4\tau_\tau$
PROPER TIME (IN τ_τ)